MONTE CARLO SIMULATIONS OF LATTICE MODELS FOR MACROMOLECULES

Kurt KREMER * and Kurt BINDER

Institut für Physik, Johannes-Gutenberg-Universität Mainz, D-6500 Mainz, Postfach 3980, Fed. Rep. Germany

1988

NORTH-HOLLAND–AMSTERDAM

Contents

1. Introduction 262
2. Simulation of single chain properties 265
2.1. Static methods 269
2.1.1. Simple Sampling (SS) 269
2.1.2. Biased Sampling or "Inversely restricted sampling" 269
2.1.3. Dimerization methods 274
2.1.4. Enrichment methods 275
2.1.5. Other methods 276
2.2. Dynamic methods 277
2.2.1. Kink-jump methods 280
2.2.2. The "Slithering Snake" ("Reptation") Algorithm 283
2.2.3. The "Wiggle" ("Pivot") Algorithm 284
2.2.4. Bond Fluctuation method 285
2.3. Grand canonical methods 286
2.4. Comparison and application 288
2.4.1. When which method? Linear chains 289
2.4.2. Confined geometries 291
2.4.3. Branched rather than linear chains 292
3. Simulation of many-chain systems 294
3.1. Methods with "Rouse" vs. "Reptation" dynamics 295
3.2. "Grand canonical" simulation of many chain systems 299
3.3. "Chain breaking" methods 301
4. Conclusion 304
References 305

Computer Physics Reports 7 (1988) 259–310
North-Holland, Amsterdam

MONTE CARLO SIMULATION OF LATTICE MODELS FOR MACROMOLECULES

Kurt KREMER * and Kurt BINDER

Institut für Physik, Johannes-Gutenberg-Universität Mainz, D-6500 Mainz, Postfach 3980, Fed. Rep. Germany

Received 18 December 1987

This article reviews various methods for the Monte Carlo simulation of models for long flexible polymer chains, namely self-avoiding random walks at various lattices. This problem belongs to the classical applications of Monte Carlo methods since more than thirty years, and numerous techniques have been devised. Nevertheless, there are still many open questions, relating to the validity of the algorithms in principle, as well as to the accuracy of the results that can be obtained in practice. This review presents a brief introduction to these problems, discusses the basic ideas on which the various algorithms are based as well as their limitations, and describes a few typical physical applications. Most emphasis is on the simulation of single, isolated chains representing macromolecules in dilute solution, but the simulation of many-chain systems is also dealt with briefly. An outlook on related problems (simulation of off-lattice chains, branched instead of linear polymers, etc.) is also given, as well as a discussion of prospects for future work.

* Now at Institut für Festkörperforschung, KFA Jülich, 5170 Jülich, Fed. Rep. Germany.

1. Introduction

In recent years macromolecules have become the basic constituents of wide varieties of materials having diverse applications in industry and daily life. Simple typical examples are polyethylene $(CH_2)_N$ and polystyrene $(CH_2CHC_6H_5)_N$. Here CH_2 ($CH_2CHC_6H_5$, respectively) is the monomer and N is the degree of polymerization, which typically is of order 10^3 to 10^5 [1].

Now a basic structural characteristic of such chain molecules is their flexibility. In a hydrocarbon chain such as polyethylene, the angle θ between successive bonds is always quite close to the tetrahedral value, $\theta = 109°$, but rotations of about $\phi = 0°$, $+120°$, $-120°$ around the neighboring C–C bond are possible (fig. 1.1a). These three angles are strongly favored because they correspond to deep minima in the rotational potential (fig. 1.1b). Note that the energy difference between the trans state and the gauche state is comparable to thermal energies; hence in thermal equilibrium a chain is not stretched out in the "all trans"-configuration, but rather the sequence of g^+, g^-, t states along the chain looks somewhat random, and globally the chain configuration resembles a random coil [1–4].

Of course, in addition to the degree of freedom ϕ for each C–C bond there is also some fluctuation in the bond angle θ as well as in the "bond length" (distance between the covalently bonded carbon atoms), but these variations are rather small and will not explicitly be considered further: the theoretical modelling of polymer configurations discussed in the present article focuses on the important qualitative aspects common to all flexible macromolecules, i.e. their

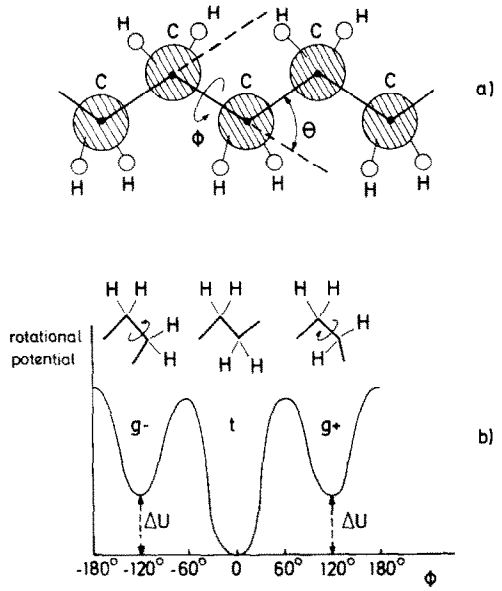

Fig. 1.1. a) Structure of a hydrocarbon polymer chain indicating the definition of bond angles θ_i and rotation angles ϕ_i. Position of hydrogen (H) atoms are shown only schematically; b) qualitative sketch of the rotational potential for alkane chains, indicating the three energetically preferred states gauche$-$(g^-), trans (t), and gauche$+$(g^+). The minimum of the trans configuration is deeper by an amount ΔU.

"universal" [3] properties such as the exponent ν in the relation between the mean-square end-to-end distance $\langle R^2 \rangle$ and the chain length (degree of polymerization) N,

$$\langle R^2 \rangle \propto N^{2\nu}. \tag{1.1}$$

In eq. (1.1), the brackets $\langle\ \rangle$ denote a thermodynamical averaging in the appropriate statistical ensemble (typically this is the canonical ensemble). In this thermal averaging not only the weighting of states in accordance with the Boltzmann factor including the rotational potential (fig. 1.1b) needs to be included, but also all other contributions to the potential energy: the monomers of the chains will interact with each other (as well as with monomers of other chains, if one considers a many chain system) and with the molecules of the solvent (if one considers polymers in solution, which is the standard case to be considered). Due to the enormous chemical variability in the local chemical structure of polymers, as well as the many possible choices of solvent, these interactions differ in detail from case to case, and moreover are seldomly known explicitly. The main feature of the effective net interaction between monomers is that it is strongly repulsive at short distance (the finite size of the monomer units leads basically to an "excluded volume"-interaction), while at somewhat larger distance in space it may be either weakly attractive or weakly repulsive, depending on the nature of the solvent. Clearly, the details of these interactions must affect the prefactor of the power law relation, eq. (1.1), but there exist arguments [3] that the exponent ν does not depend on the parameters describing these interactions: rather there are wide "classes" of behavior for which ν takes a "universal" value, in the limit $N \to \infty$. The square root of the prefactor can be interpreted as the persistence length or the Kuhn step length of the specific polymer.

Eq. (1.1) is only one example for a law involving a universal exponent. A second universal exponent arises when one considers the configurational entropy of the chain, or a related quantity, the partition function of a single chain. Asymptotically it is described by [3]

$$Z_N \propto N^{\gamma-1} q_{\text{eff}}^N, \quad N \to \infty, \tag{1.2}$$

where γ is another universal exponent while q_{eff} is a non-universal quantity (depending on temperature, for instance). As an example, consider the "rotational isomeric state" (RIS) model [2] which follows from fig. 1.1 when we restrict ϕ to precisely the three choices $\phi = 0, \pm 120°$ and take only the rotational potential into account but neglect all other interactions: then the chain partition function factorizes in a product of the partition functions $q_{\text{eff}} = 1 + 2\exp(-\Delta U/k_B T)$ for each C–C bond, ΔU being the energy difference between the trans (t) and gauche (g^+, g^-) configurations, $Z_N = (q_{\text{eff}})^N$, and hence $\gamma = 1$. It turns out, however, that considering excluded volume interactions one still finds a result of the form eq. (1.2) but now γ exceeds unity.

In view of the fact that a detailed and realistic molecular description in most cases is not possible due to incomplete knowledge of intermolecular potentials and is not even required if the calculation of universal properties is desired, it is common and legitimate to consider simple models which capture the essential physics of the problem: these models are chosen such that they yield the same "universal" properties as the real material, but otherwise they are not microscopically realistic, rather their choice is dictated by computational convenience. Such a

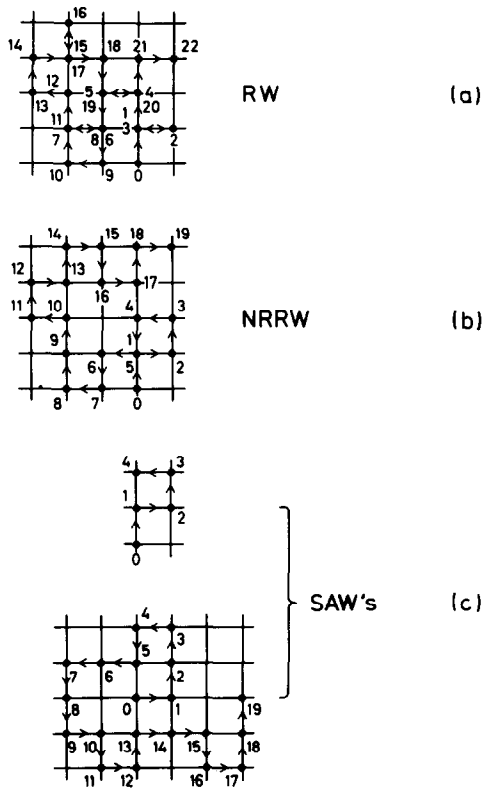

Fig. 1.2. (a) construction of a 22 step random walk (RW) on the square lattice; (b) same as a) but for a non-reversal-random walk (NRRW); (c) two examples of self-avoiding walks (SAW's).

model for macromolecular configurations is the *self-avoiding walk* (SAW) on a lattice (fig. 1.2c). The idea of simulating polymers on a lattice, however, is much older than any knowledge of universality. Already in the early fifties Montroll [5] and King [6] performed the first simulations. Each site of the lattice which is occupied by the walk may correspond to a monomer, and the lattice bond connecting two subsequent steps of the walk may be pictured as a C–C bond in the above more realistic examples. Just as in the RIS model there are three choices for each bond, in the SAW model there are $q-1$ choices to be considered at each step of the walk, if the lattice has coordination number q. If we would disregard excluded-volume interactions completely, we would rather consider a simple random walk (RW), which is allowed both to intersect itself and to backfold on itself (fig. 1.2a). As a model of polymer configurations in dilute solution, the RW which trivially yields $\nu = \frac{1}{2}$ is not realistic. A variant of the RW is the "non-reversal random walk" (NRRW), which is still allowed to intersect itself itself in loop-like configurations (fig. 1.2b), but is not allowed to backfold on itself. We simply have for the partition functions of these walks

$$Z_N^{\mathrm{RW}} = q^N, \quad Z_N^{\mathrm{NRRW}} = (q-1)^N. \tag{1.3}$$

Thus for the tetrahedral lattice ($q = 4$) Z_N^{NRRW} is the same as Z_N for the RIS model with $\Delta U = 0$.

Since the tetrahedral lattice describes the rigid bond angle of alkane chains realistically, it enjoys great popularity as a lattice for the simulation of polymer models; other popular lattices are the simple cubic (sc) and face-centered cubic (fcc) lattice, of course, as well as simple two-dimensional lattices (square (sq), triangular (t)). The choice of the lattice is somewhat arbitrary, since the universal properties depend only on its dimensionality. Thus typically the selection is governed by computational convenience. Not only Z_N^{NRRW} can be calculated exactly, but also all configurational averagess [such as the one considered in eq. (1.1)] can be obtain exactly as well [7]. Thus the NRRW is a nice testing model for Monte Carlo programs, where one omits in a SAW program the SAW restriction to check other parts of the code (including the quality of pseudorandom numbers, the judgement of statistical accuracy obtained, etc.): apart from exact enumerations of very short SAW's ($N \leqslant 20$, e.g. ref. [8], some of the classic papers even use only $N \leqslant 10$, e.g. ref. [9]), there are hardly any exact results for SAW's on three-dimensional lattices. This lack of exact results for long SAW's is one of the reasons why the judgement of the validity, accuracy and efficiency of the various algorithms proposed for the Monte Carlo study of SAW's is still a difficult problem. Fig. 1.3 now gives an illustration of the kind of systems which can be analyzed by the methods discussed in the present review.

The present review now does not aim to discuss the physical problems that have been clarified by such Monte Carlo simulations [10,11], but rather to describe the basic ideas involved in the various algorithms that have been proposed for the study of SAW's, and to critically compare them. Most of this article (section 2) deals with the simulation of single-chain properties, since we feel that the simulation of many-chain systems (section 3) is still in its early stages. A general discussion including the outlook on unsolved questions will be presented together with our conclusions (section 4).

In our next section, we start with a more detailed description of single chain properties. Then we discuss static methods (section 2.1) such as the construction of chains via "simple sampling", related biased sampling methods as well as chain fusion methods and other approaches. In section 2.3 we discuss several grand canonical algorithms for single chains where the number of bonds N per chain is not conserved and leads to an average chain length $\langle N \rangle$. Dynamic methods, such as the "kink-jump"-method (fig. 1.4a), the "slithering snake"- (or "reptation"-) method (fig. 1.4b) or the "pivot"- (or "wiggle"-) algorithm (fig. 1.4c) will be discussed in section 2.2 as well as the bond length fluctuation algorithm (fig. 1.4d), while section 2.4 contains a comparison of these methods and discusses specific applications (constrained geometries, etc.) and extensions (such as branched chains rather than linear polymers, etc.).

2. Simulation of single polymer chain properties

Monte Carlo methods for a long time were the only way to yield direct information on polymers having a large ($N > 20$) number of bonds. Enumerations typically were confined to $N \leqslant 20$. Long before the renormalization group methods established the principle of universality of critical exponents, Monte Carlo data strongly suggested this. For reviews on this early and pioneering role of Monte Carlo simulations we refer to ref. [11].

Before we start to describe the various algorithms, we shortly review the typical properties of single isolated polymer chains. It would be beyond the scope of the present article to give a

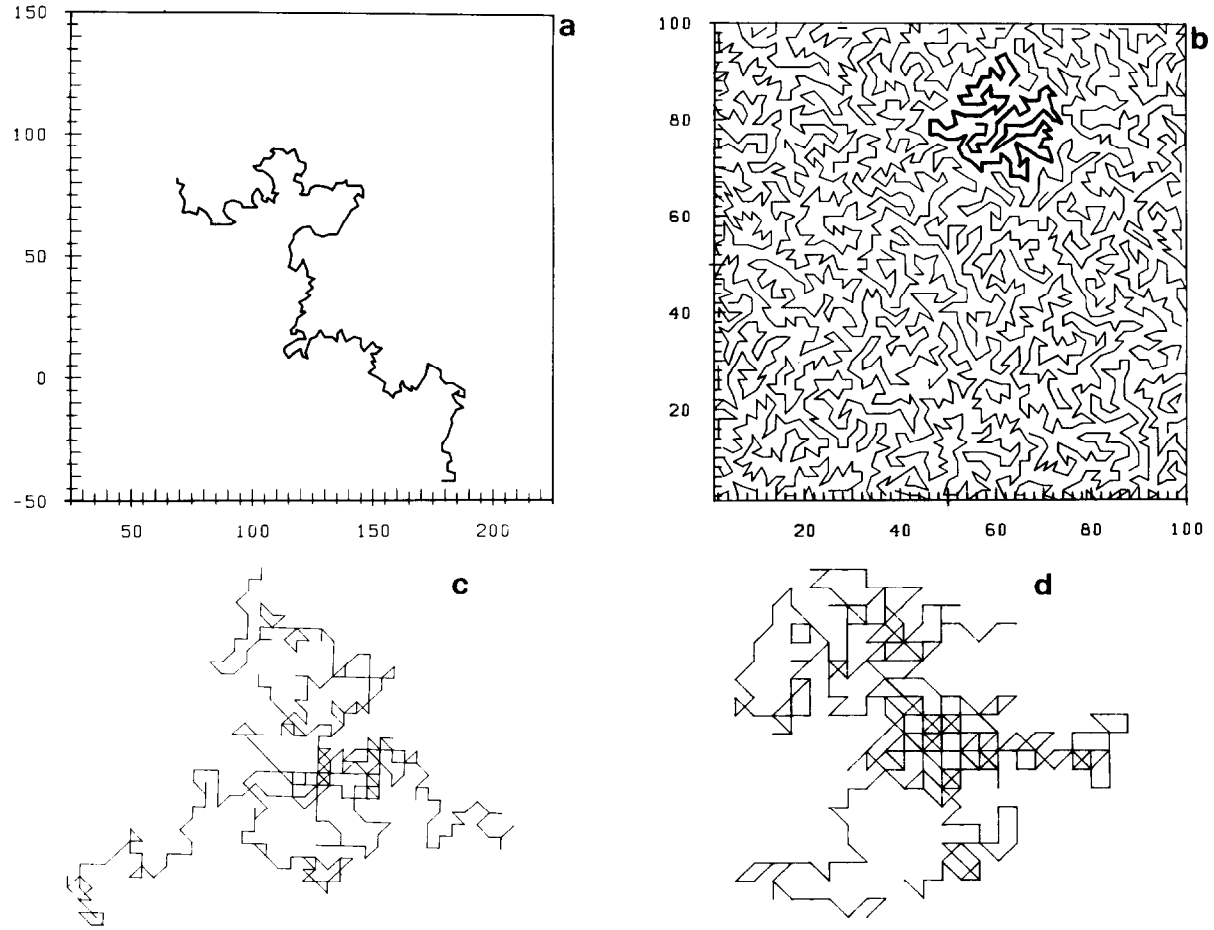

Fig. 1.3. Four typical snapshots of simulated polymers. (a) 2-d SAW of length $N = 200$ (from ref. [131]); (b) a 2-d melt at 80% density, the chains started in a stretched configuration, as one can see the configuration is almost relaxed; (c) a projection of a 3-d star of $f = 6$ arms of $N = 60$ bonds each in (c) good solvent and (d) θ-solvent (from ref. [66]).

detailed description, however, there exist excellent references on the topic [1–3,12]. As mentioned in the introduction, the qualitative properties of polymers do not depend on the special chemical species. This "universality" was discovered by the Gennes in 1972 [13]. For a general review of such scaling properties we refer to ref. [3]. Here we describe some of the universal features which are needed to discuss the various Monte Carlo methods. For simplicity already here we confine our discussion to lattice models.

As mentioned in the introduction, one can model a polymer as a simple SAW on a lattice. The only interaction considered is that two "monomers" are not allowed to occupy the same lattice site. Let q be the coordination number of the lattice. Then we have for the number of SAW's of length N Z_N [3]

$$Z_N \propto q_{\text{eff}}^N N^{\gamma-1}, \tag{2.1}$$

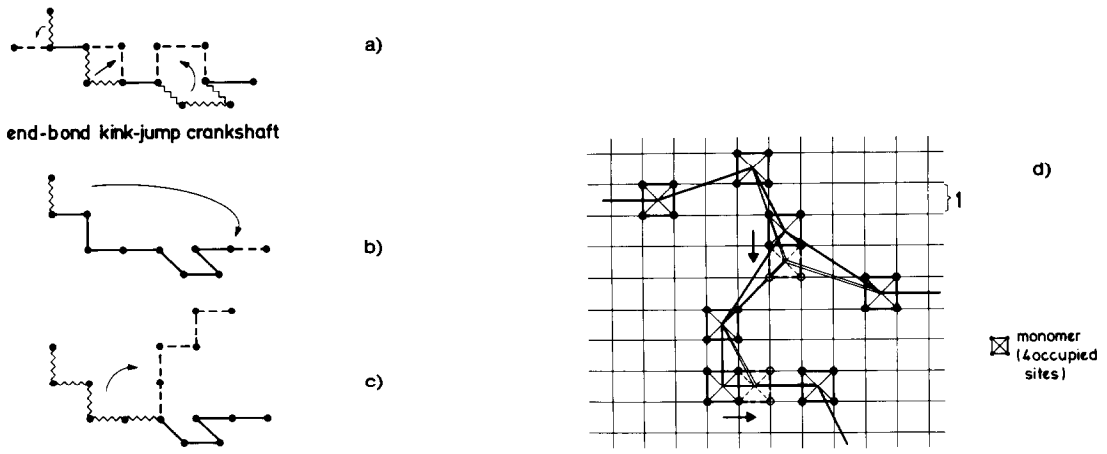

Fig. 1.4. Various examples of dynamic Monte Carlo algorithms for SAW's: bonds indicated as wavy lines are moved to new positions (broken lines), other bonds are not moved. a) Generalized Verdier–Stockmayer algorithm on the simple cubic lattice showing three types of motions: end-bond motion, kink-jump motion, crankshaft motion; b) "slithering snake"-("reptation"-) algorithm; c) "pivot"-("wiggle"-) algorithm; d) bond length fluctuation algorithm on the square lattice. Each monomer blocks four sites around its center from occupation by other monomers. The bond length is allowed to fluctuation from a minimum value of $\sqrt{4}$ to a maximum value of $\sqrt{13}$ lattice spacings in the example shown which refers to three-arm star, where also the center is able to move as indicated in the figure.

γ is a critical exponent with $\gamma \approx 7/6$ ($d = 3$), $\gamma = 1$ ($d \geqslant 4$) [3] and $\gamma = \frac{32}{43}$ ($d = 2$) [14]. q_{eff} is the effective coordination number (or inverse coupling constant in the magnetic language [13]) with

$$q_{\text{eff}} < q - 1. \tag{2.2}$$

Note that Z_N just gives the number of different embeddings of a non-intersecting path of N steps on a lattice. For polymeric systems, this corresponds to an isolated chain in a good solvent. One can think of the solvent as the empty lattice sites. The net interaction of solvent–solvent, chain–solvent and chain–chain is summarized in the excluded volume between the monomers. Eqs. (2.1) and (2.2) already display one of the main difficulties one has to overcome. There exist $q(q-1)^{N-1}$ NRRW's of length N starting at a given point of the lattice. However, only of the order of $N^{\gamma-1}\,(q_{\text{eff}}/(q-1))^N(q-1)/q$ out of all NRRW's are self-avoiding. Thus the probability to find a SAW by simply generating a NRRW decays exponential. This is the so-called chain attrition problem. In table 1 we give a list of q_{eff} for various lattices. Note that each walk has exactly the same probability!

But not only the partition function Z_N is of interest, especially since it cannot directly be measured. Typical other physical quantities are the mean square end-to-end distance

$$\langle R^2(N)\rangle = \left\langle (\boldsymbol{r}_0 - \boldsymbol{r}_N)^2 \right\rangle \propto N^{2\nu} \tag{2.3a}$$

and the radius of gyration

$$\left\langle R_{\text{G}}^2(N)\right\rangle = \frac{1}{N+1}\left\langle \left(\sum_{i=0}^{N} \boldsymbol{r}_i - \left(\frac{1}{N+1}\sum_i \boldsymbol{r}_i \right) \right)^2 \right\rangle \propto N^{2\nu}. \tag{2.3b}$$

Both have the same asymptotic power law [3] with $\nu = 3/4$, $d = 2$ [14], $\nu \approx 0.588$, $d = 3$ [15] and $\nu = 1/2$, $d \geq 4$ [3]. For RW's it can be shown that $\langle R^2(N)\rangle / \langle R_G^2(N)\rangle = 6$ [1]. The radius of gyration is of special interest, since it can be measured directly from the structure function. Eq. (2.3) leads us to another serious problem which we shortly discuss for RW's in $d = 3$. For RW's one trivially finds $\langle R^2(N)\rangle = \ell^2 N$, where ℓ is the lattice constant. For $N \gg 1$ the distribution of the end-to-end vector is a Gaussian with [12]

$$P(\boldsymbol{R}) = \left(\frac{3}{2\pi \ell^2 N}\right)^{3/2} \exp\left(-\tfrac{3}{2}\boldsymbol{R}^2/\ell^2 N\right). \tag{2.4}$$

The width is just $\langle R^2(N)\rangle$. Now for the fluctuation in R^2 this gives

$$\Delta_R = \frac{1}{\langle R^2\rangle}\sqrt{\langle R^4\rangle - \langle R^2\rangle^2} = \sqrt{2/3} \tag{2.5}$$

which describes a serious problem. Usually for measurable quantities the variance Δ_R decreases with increasing system size, while this is not the case here. Such typical problems with the lack of self-averaging where also found for other systems and can lead to serious complications in the course of a simulation [16]. For the radius of gyration Δ_{R_G} also is not zero although smaller than Δ_R. For SAW's $P(\boldsymbol{R})$ is not known exactly [3,12], however, one has the scaling form

$$P(\boldsymbol{R}) = N^{-d\nu} f(R/N^{\nu}). \tag{2.6}$$

Again Δ_R, Δ_{R_G} do not vanish (e.g. $\Delta_R \approx 0.70$, $\Delta_{R_G} \approx 0.405$, $d = 3$ [17]). For the actual simulation this means that the relative error for the determination of R^2, R_G^2 is $\Delta_{R,R_G}/\sqrt{\text{number of generated chains}}$. Roughly speaking, we need as many long chains as short chains in order to obtain the same relative accuracy! In view of the attrition this becomes a serious problem.

Up to now only pure SAW's were considered. However, polymer physics is not confined to the good solvent case. Of special interest are θ-solutions [1–3,12]. Here the solvent–monomer repulsion leads to a net attraction between the chain monomers. Exactly at θ the SAW condition and this attraction just cancel each other in a way that the chains display random walk exponents. In the phase transition language the θ-point is a tricritical point, where $d = 3$ is the upper critical dimension [3]. This leads to mean field exponents $\nu = 1/2$, $\gamma = 1$ for $d = 3$ [1,3,18,19]. Physically this also means that the second virial coefficient between two chains vanishes [20], however the binary cluster integral between monomers is already negative [19,21,22]. For even lower temperatures (stronger attraction) the chains collapse giving $\nu = 1/d$. For $d = 2$ the situation is more complicated, no precise estimate of ν is available at θ (see section 2.1.2). For a more detailed description of the physical properties of single polymer chains, we refer to the cited books [1–3,12] and the subsequently referenced publications.

We first review now the static methods where chains are constructed by some mechanism and each new chain is statistically independent from the previous one (subsection 2.1), then we consider the dynamical methods (subsection 2.2) and the various grand canonical algorithms (subsection 2.3). Finally, we discuss special cases and compare the applicability of the methods (subsection 2.4).

2.1. Static methods

Static methods generate polymer chains by constructing walks either step by step or by bigger units. Each successfully constructed chain is statistically independent from the previous one, since each time one starts from the very beginning. One advantage is that not only the chains of the desired length can be analyzed but also all shorter polymers, which occur in the course of the run, can be used.

2.1.1. Simple Sampling (SS)

The SS method was the first Monte Carlo method used for polymers [5,6,11,23]. Consider a lattice with coordination number q. We want to generate chains with up to N steps. The chain starts at the origin. The first step is chosen randomly out of the q directions. The subsequent steps are then with equal probability taken out of the $q_0 = q - 1$ possible directions, where a direct backfolding is forbidden. As soon as the walker, let us say at step i, tries to jump onto an already occupied site, one has to start with a *completely new* chain. Only the previous $i - 1$ steps can be used to study walks of length 1 to $i - 1$. To generate the next chain we have again to start at $i = 1$! By this trivially the requirement that each walk of a given length has to have the same probability is fulfilled [12,24]. This method is the most simple and direct approach to simulate polymer chains on a lattice. Note that all other methods of going back only a certain number of steps (see e.g. ref. [26]) lead to a bias which produces a different statistical system! The only exceptions are chain fusion methods with special break points as discussed later. Clearly this method has certain advantages. In one run configurations over a broad range of chain lengths are generated. Different configurations are statistically independent, allowing for a standard analysis of the error. (Remark: The sample of shorter chains is of course statistically linked to the long ones.) For $\langle R^2 \rangle$ e.g. we then have $\langle \Delta R^2(N) \rangle = \Delta_R/(\text{number of chains})^{1/2}$. The success rate σ_N directly gives the partition function, namely

$$\sigma_N = \frac{Z_N}{q(q-1)^{N-1}} \propto \left(\frac{q_{\text{eff}}}{q-1}\right)^N \left(\frac{q-1}{q}\right) N^{\gamma-1}. \tag{2.7}$$

However, this also illustrates the main disadvantage. Since σ_N decays exponentially, it is very expensive to generate long chains. For example we find for the fcc lattice $\sigma_{100} = 0.0022$ [27] while on the square lattice $\sigma_{48} = 0.07$ [28]. The literature usually defines $\lambda = -\ln q_{\text{eff}}/(q-1)$ as the attrition constant. Values for λ for various lattices are given in table 1. Although this is the first method which was used, it still is very useful to generate relatively short chains [21,29] which are then used for subsequent calculations.

2.1.2. Biased Sampling or "Inversely Restricted Sampling"

The first attempt to overcome the attrition was the biased sampling idea of Rosenbluth and Rosenbluth [30] and Hammersley and Morton [31] some 30 years ago. They originally called it inversely restricted sampling. Fig. 2.1 compares the construction of a biased chain with simple sampling chain. The procedure is as follows (a description for continuum chains can be found in ref. [32]): Consider a SAW of i steps on a q-coordination number lattice. To add the $(i+1)$st step we first check which of the $q_0 = q - 1$ SS jump sites is empty. If $k (q_0 \geq k > 0)$ sites are

Table 1
Effective coordination number q_{eff} and attrition constant λ for various two and three dimensional lattices. The data are taken from an enumeration study using Padé approximations by Watts [25]. This paper also contains a rather complete list of earlier enumeration studies. The ref. gives $q_{\text{eff}} \cdot \lambda$ is then given by $\lambda = -\ln q_{\text{eff}}/(q-1)$. The brackets for the data of q_{eff} gives the variation of the data of ref. [25]

		q_{eff}	q	λ
$d=2$	honeycomb	1.8478(3)	3	0.07915
	square	2.6385(3)	4	0.12840
	triangle	4.1520(10)	6	0.18585
$d=3$	diamond	2.8790(10)	4	0.04117
	sc	4.6835(10)	6	0.06539
	bcc	6.5295(10)	8	0.06958
	fcc	10.035 (2)	12	0.0918

empty one takes one of these with equal probability $1/k$, if k is 0 the walk is terminated and we start from the beginning. This reduces the attrition dramatically. Now each N step walk has a probability $P_N(\{r_i\}) = \prod_{i=1}^{N}(k_i)^{-1}$. Thus dense configurations are clearly more probable. This bias one has to correct for, in order to generate the sample of equally probable walks. To compensate for the bias, each chain does not count as 1 in the sample but with a weight

$$W_N(\{r_i\}) = \prod_{i=1}^{N} k_i/q_0. \tag{2.8}$$

Using 2.8 we have $P_N(\{r_i\})W_N(\{r_i\}) = q_0^{-N}$. Of course, this procedure samples exactly the same configuration space as the SS method. The only difference originates in the probabilities of the chains. For the square lattice, e.g. at $N = 200$ still 70% [33] of the attempts to built the chain are successful while for $d = 3$ at $N = 700$ 90% (diamond lattice) [33] and 93.3% (fcc lattice) [27] of the attempts survive. This explains that the use of this method is appealing and many investigations (see refs. in ref. [27]) tried to take advantage of it. However, one has to be extremely careful as the subsequent discussion shows. Batoulis and Kremer [27] performed a detailed analysis of the statistical properties of biased sampling methods. They use the fact that the statistical weight of the chain is directly connected to the nearest neighbor contacts. (Indeed for the honeycomb lattice one can map the bias on an attractive nearest neighbor potential [34].) The bias introduces an effective attraction among the monomers. This also leads to a systematic

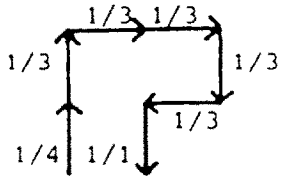

Fig. 2.1. Construction of a SAW on the square lattice. The probabilities are given for each step for the biased sampling procedure. For SS all probabilities are $1/(q-1)$.

error [35] towards more compact walks. However, this systematic error is small compared to the statistical one of a sample of many thousands of chains! Thus we here constrain ourselves to the statistical problem. We discuss this for the partition function. The idea which is mean field like is that the neighbor contacts are assumed to be homogeneously distributed along the chain. Then eq. (2.8) reads

$$W_N(\{r_i\}) = \prod_{i=1}^{N} \frac{k_i}{q_0} = \prod_{i=1}^{N} \left(1 - \frac{m_i}{q_0}\right) \approx \prod_{i=1}^{N} \left(1 - \frac{\langle m(\{r_i\})\rangle}{q_0}\right), \tag{2.9}$$

$m_i = q_0 - k_i$ is the number of occupied neighbors and $\langle m(\{r_i\})\rangle$ is the average energy (nearest neighbor contacts) per bond of configuration $\{r_i\}$. Using this one finds that

$$\ln W_N(\{r_i\}) \propto \langle m(\{r_i\})\rangle. \tag{2.10}$$

This directly leads to the arguments of ref. [27]. The average of the logarithm of the weights is proportional to the nearest neighbor energy of the chain.

For both of the corrected and the uncorrected walk the energy is an extensive quantity where the constant of proportionality is different for the two cases. Uncorrected walk here means that the chain is sampled by biased sampling but the weights are always set to be one. The width of the energy distribution, however, only grows with $\sqrt{N}$ since this is the square root of the heat capacity $C = (1/T^2)(\langle E^2\rangle - \langle E\rangle^2)$. E equals the nearest neighbor contacts. Therefore the distributions of the contacts run apart proportional to N while the width only grows like $\sqrt{N}$. The consequence is that the most relevant configurations, generated by biased sampling are pushed to the very ends of the distribution function. Using this, Batoulis and Kremer [27] derive an analytic expression for the quality of the standard biased sampling method. With n_{SS} a number of simple sampling chains, then n_{BS} is the number of biased sampling chains of same length needed to obtain the same relative accuracy. They find for the ratio

$$\begin{aligned} x &= \frac{n_{BS}}{n_{RR}} = \exp(-S^2), \\ S^2 &= \left\langle \ln^2 W_N(\{r_i\})\right\rangle - \langle \ln W_N(\{r_i\})\rangle^2, \end{aligned} \tag{2.11}$$

for the accuracy of the partition function.

For the fcc lattice one has $S \approx (9.5N - 630)^{1/2}/q_0$. Fig. 2.2 shows a plot of $\langle R^2\rangle$ and $\langle R_G^2\rangle$ as well as the calculated and "measured" errors for the partition function. For the other quantities (e.g. $\langle R^2\rangle$, $\langle R_G^2\rangle$) a similar relation holds.

If one uses the biased sampling approach, one has to take care that the bias which one introduces is a bias towards the desired physical situation. This can be used e.g. for constrained geometries (see subsection 2.4.2) or, e.g. for the analysis of the θ-point. Several authors [20,36–38] used this approach to analyze the θ-point and the corresponding collapse transition. To do so one has to store the quantities of interest with respect to their contact distribution. Then the chains are weighted by a Boltzmann factor $\exp(-E/k_BT)$. By this method it is possible to analyze several temperatures from the same sample as was done from SS samples [21] and biased samples [20,36–38]. It is clear that the data are at their best, when the Boltzmann factor is

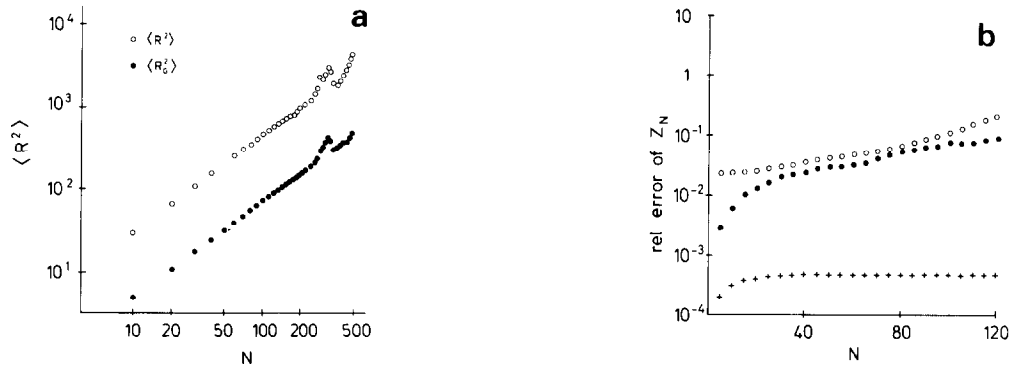

Fig. 2.2. (a) Squared radius of gyration and end to end distance for chains on the fcc lattice for 32768 chains of each length. The chains were generated by biased sampling; (b) error of the partition function for 2048 chains of each length. (+) SS chains, (●) biased sampling chains, (○) calculated error due to eq. (2.11). Both figures are taken from ref. [27].

about to cancel in average the weighting due to the bias. As has been investigated in detail, biased sampling introduces an attraction which is slightly weaker than required for the θ temperature in $d = 3$ [33,34,39]. Therefore, this method seems to be the natural approach to study the θ-point. For $d = 2$ the situation is not that clear. One does not know exactly the critical exponents at θ and there still is some discussion about it [40]. For biased sampling on a square lattice it turns out that the weight distribution is too narrow to analyze a temperature regime which is broad enough to arrive at precise results [41]. Birshtein et al. [42] use a different approach. Since for $d = 2$ even for biased sampling many chains run into cages, they construct their chain by biased sampling plus the constraint that the walker is not allowed to run into cages. This model, the so-called indefinitely growing SAW (IGSAW), was discussed in a different context as a model in its own [43]. This method, however, leads to a different set of possible configurations than biased sampling or SS. One can argue that this IGSAW procedure only samples the ends of infinite chains and consequently should lead to the right results for large N. It is not completely clear how this affects the results for finite systems. Biased sampling was also used to study the phase diagram of semidilute polymers [44].

Modifications and extensions

Since the above mentioned problems sometimes may lead to serious mistakes, several modifications were proposed. The aim always is to introduce a bias which samples as exactly as possible the configurations which are dominant in the physical system under investigation. One direct extension is the soft bias [45–47]. Here at each step one devides the q_0 SS-jump sites into n^+ preferred and n^- not preferred directions. By introducing a bias factor Q one chooses with probability $p^+ = Q/(n^+Q + n^-)$ an n^+ site and $p^- = 1/(N^+Q + n^-)$ an n^- site. The weights then are changed to $W^+(n^+, n^-) = (Qn^+ + n^-)/Q(n^+ + n^-)$ and $W^-(n^+, n^-) = (Qn^+ + n^-)/(n^+ + n^-)$ respectively, depending on the choice. By varying Q one can smoothly go from SS ($Q = 1$) to biased sampling ($Q = \infty$). Typical applications are constraint geometries (see subsection 2.4.2). A different modification is the extended biased sampling [27,48]. There the walk again is constructed by a one step process. The difference is that at each step i one looks more than one step (e.g. to $i + 2$) ahead and proceeds with the walker into a direction where the

probability is given by the number of empty sites for the $(i+2)$nd step. This modifies the bias and allows to generate longer chains. This was already (with a slight modification, as discussed below) proposed in 1957 by Wall et al. [48]. They realized that the main contribution to the chain comes from the smallest loops. For the square lattice, they proposed a way of adding four steps at once where all possible four step walks where stored. By knowing the possible pairs of four step walks they were able to construct large chains. Since the number of possible additions depends on the previous four step part, the different walks again have different probabilities. Of course they correct for this bias. Note that, since the problem of smallest loops is eliminated, the typical bias is much weaker than for standard biased sampling.

A related idea was used in the scanning future step method of Meirovitch [49–51]. He again goes back to one step growth, however, looks more than one step ahead. The procedure was influenced by the idea of counting walks. Let us construct a walk of length N. Further let us assume we already have $k-1$ steps. If $\nu = 1, \ldots, q$ is one of the lattice directions, the probability for step k to proceed in direction ν $p_k(\nu \mid \nu_1, \nu_2, \ldots, \nu_{k-1})$ then given by

$$p_k(\nu \mid \nu_1, \nu_2, \ldots \nu_{k-1}) = \frac{M_\nu(k, N)}{M(k, N)}. \tag{2.12}$$

$M_\nu(k, N)$ is the number of all possible ways to complete the walk up to N through direction ν, while $M(k, N) = \Sigma_\nu M_\nu(k, N)$. This leads to a random selection of walks out of all the possible ones via the recursion relation (2.12). To do this one needs the knowledge of all walks. This is not the case in practice. Meirovitch now introduces the "approximate scanning method '[' [49–51] by only looking $b \leqslant N-(k-1)$ steps ahead. However, now not all walks have the same probability any longer. Thus the overall probability in $P(\{r_i\}, b)$ is given by

$$P(\{r_i\}, b) = q^{-1} \prod_{k=2}^{N} P_k(\nu \mid \nu_1, \nu_2, \ldots, \nu_{k-1}; b). \tag{2.13}$$

Without correcting for the bias this becomes an exact MC procedure for $b = N-(k-1)$. For $b = 1$ the standard biased sampling would be recovered and for $b = 2$ this would be the extended biased sampling as discussed above. The correction of the bias, is called importance sampling. Practically $b \leqslant 8$ for $d = 2$ and $b \leqslant 4$ for $d = 3$. Since the bigger b the smaller the introduced bias is, the procedure converges to the standard SAW results. This method was also used [52] for the calculation of the osmotic pressure of semidilute solutions and for chains in constrained geometries [53]. To correct for the bias in a phenomenological way, Meirovitch later [54] introduced his "mean field scanning methods". Here the probabilities for each step are modified by

$$P_k(\nu \mid \nu_1, \nu_2, \ldots \nu_{k-1}) = M_\nu(k, b) m^{-e_\nu x_0} / \sum_\nu M_\nu(k, b) m^{-e_\nu x_0}, \tag{2.14}$$

e_ν is the unit bond vector in direction ν while x_0 is the unit vector pointing from the center of gravity of the preceding part of the chain to the origin of step k. For $m < 1$ this leads to an extension of the walk. His argument is that the best choice of m, which is called m^*, leads to the smallest fluctuations in entropy, since for the unbiased walks each walk has exactly the same

probability leaving no fluctuation in the entropy. Note that this procedure does not reduce the bias in the sense of correcting weights, but tries to push the sampling procedure towards a direct generation of unbiased walks. Since m^* turns out to be strongly N-dependent, it is difficult to give a rigorous estimate of the properties of this approach. A combination of all the above modifications on the scanning method plus an acceptance criterion for the walks due to the "generalized MC approach" of Schmidt [55] was recently used for selfinteracting random walks [56]. The philosophy here is to perform a Metropolis sampling (see subsection 2.2) for the acceptance of a generated chain. The chains are generated by the above method. The ratio of the probabilities then plays the role of the ratio of the Boltzmann factor of ordinary importance sampling. For details of the Metropolis sampling see subsection 2.2. This method no longer suffers from unknown systematic errors but again it will work well in practice only if the acceptance rate is not too low.

2.1.3. Dimerization methods

Up to now we discussed methods where the walks were constructed step by step in a consecutive way. All these approaches share the problem of a finite attrition constant λ or a strongly biased distribution function for the various physical quantities. A completely different idea, which leads to $\lambda = 0$ without introducing a bias was proposed some time ago by Alexandrovicz [57] and Suzuki [58]. The idea to overcome attrition here is to assemble long chains out of successfully generated short chains. To describe the method one can use modern scaling ideas. However, when originally invented, knowledge of scaling was very rudimentary. Here we follow the scaling picture [59] for the binary assembly case. Let us assume that we have two walks of size $N/2$. Both are supposed to be uncorrelated. Since both walks are taken out of the $Z_{N/2} = q_{\text{eff}}^{N/2}(N/2)^{\gamma-1}$ different configurations, the probability that they form one of the Z_N SAW's of N steps $P_{\text{BIN}}(N)$ is simply

$$P_{\text{BIN}}(N) = Z_N/(Z_{N/2})^2 = N^{\gamma-1}/(N/2)^{2(\gamma-1)} = 2^{2(\gamma-1)}N^{-(\gamma-1)}. \tag{2.15a}$$

Thus the acceptance rate is a direct measure of the exponent γ. This procedure now can be iterated. Since the acceptance rate decreases only with a power of N the attrition constant λ is equal to zero. From this it is also evident that the binary assembly with doubling the chain length is the most economic way because it is easier to generate two chains of $N/2$ instead of an asymmetric pair. Fig. 2.3 illustrates the procedure.

If is easy to estimate the computational effort of such a procedure. Here this is done for the chain doubling. If we measure the computing time in operations like calculating a distance etc., the time to combine a walk is proportional to N. With the acceptance probability this gives the recursion equation for the time $T(N)$ to construct a walk of length $(2N)$ (with k, k' constants)

$$\left.\begin{aligned} &T(2N) = k'(kT(N) + N)N^{\gamma-1} + k'kT(N)N^{\gamma-1} + k'N^{\gamma}. \\ &\text{This leads to [60]} \\ &T(N) \propto N^{((\gamma-1)/2)\log_2 N}N^{(1-\gamma)/2} \end{aligned}\right\} \tag{2.15b}$$

for the computing time needed. The prefactor then is, e.g. a function of the initial chainlength used. Thus the time required to generate a chain by dimerization grows only with $N^{c\log_2 N}$

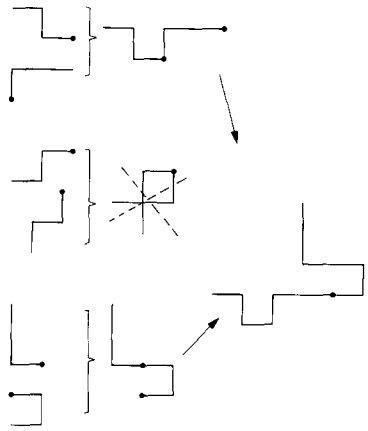

Fig. 2.3. Schematic illustration of the dimerization procedure. Starting from the 3-step walks a 9-step walk is generated. Note that the source of partial walks at each step has to contain all possible configurations!

instead of exponentially with N. This method was used for SAW's by Alexandrovicz and Accad [61]. They then extended the approach to the Domb Joyce model [62,63]. A more general approach was used for continuous spatial dimensions d with $1 < d \leqslant 4$ [64]. A very direct use of these ideas was proposed recently by Batoulis [65]. Suppose we generate a chain of length $N/2$ by a SS procedure. One simply continues for the second $N/2$. However, when the second half is not selfavoiding for itself, one again starts at the middle. Only when the SAW condition between the two halfs is violated but not for the second half itself one has to start at the very beginning. The procedure then is iterated. This also helps to overcome the relatively complicated book-keeping procedures for the initially generated walks and one automatically takes the partial walks out of the whole set of configurations. For the computing time the same asymptotic law is reached. Since the time from checking the overlap between the two partial chains is incorporated in the construction of each partial chain eq. (2.15) reads $T(2N) = k'kT(N)N^{\gamma-1}$. Thus this approach is especially useful, if one wants to generate many relatively long walks, as, e.g. done for stars [66]. Chen [67] used a dimerization method to generate ring polymers, while Madras and Sokal [60] used the dimerization to construct the initial states for their simulation with the pivot algorithm (see subsection 2.2.3).

2.1.4. Enrichment methods

The enrichment method [68] is one of the first modifications of SS or biased sampling, already containing some of the ideas of the latter developments. This early development lead to one of the very first intriguing successes of Monte Carlo methods. Wall and Erpenbeck presented already 1959 [68], for those times, excellent numerical evidence for the exponent ν to be 0.59 ($d = 3$) and 0.75 ($d = 2$). The authors tried to overcome the sample attrition by using successfully generated short walks of length s more than once, say p times. The price they pay is that the chains are not statistically completely independent. Once a walk of s steps successfully is generated by the SS method. Now one tries to continue this chain up to $2s$ in p different (chosen by SS) ways. Then the number N_{2s} of $2s$-step chains is

$$N_{2s} = pN_s \exp(-\lambda s) \tag{2.16}$$

with λ the attrition constant. This process then is continued for blocks of s steps up to the desired chain length. The authors fix p ahead in order to avoid a bias. Any configuration dependent choice of p of course would introduce a bias. This very much reminds of the enumeration procedure where the steps are substituted by the s-step chains and the enumeration of the new steps by the SS of the s-step additions. For this procedure the obtained chains are not statistically independent. Taking $p \ll \exp(+\lambda s)$ would lead to the typical SS problems, while $p > \exp(+\lambda s)$ would lead to an exploding sample of highly correlated walks. The authors argue that the best choice for p is to compensate the attrition exactly, giving $p = \exp(\lambda s)$. Note that this sampling gives equal probability to every generated walk. At each start of a hierarchy of walks only a small part of the configuration space is possible to sample by the enrichment restriction, however, these parts are equally probable giving the altogether unbiased sample. Lax and Gillis [69] used this method for an extensive study of the Domb Joyce model [63]. A comparative study of different values of $g = p \exp(-\lambda s)$ showed that values of $g > 1$ lead to strongly correlated samples with a systematic tendency towards an increase in the overall dimensions of the chains [70].

2.1.5. Other methods

In the course of the Monte Carlo investigation of polymers many specified models trying to comply with the chemical structure of a given chemical species were discussed. It is beyond the scope of the present review to discuss all these attempts. Here we try to cover such methods which are of more general importance to investigate qualitative properties. One line of research was to vary the effective excluded volume. This can be done either by using different lattices or introducing interactions, as described in the previous chapter. Without a nearest neighbor interaction this was done by Wall et al. [71]. They introduce a bias towards trans configurations. This made short loops less probable. They also argued that this better corresponds to a polymer structure. However, in the light of the scaling theories we know, that this only influences the persistence length. Barrett and Pound [72] introduced a high coordination number SAW model where the bonds on the square lattice can reach all lattice points in a distance $\sqrt{3}$ from the origin. While in principle the same statements as above hold for this approach, it is interesting with respect to branched polymers confined to lattices (see subsection 2.4.3) [73]. Smith [74] tried to model SAW's by the "sliding segment" method. He sampled walks by the SS method where the SAW condition for each monomer only was encountered by the R neighbors along the chain ($R/2$ neighbors for end monomers). His argument was that the dominant interaction comes from short loops and thus $R \approx 100$ should be sufficient. However, it was shown earlier that for $N \gg R$ the walk again has RW structure [5,75].

A different method was used by Hammersley and Morton [76] for $d = 2$. They started out with the standard biased samples method. When a chain ran into a cage the walk was not terminated but a certain number of steps was removed in order to continue the chain. This introduced a bias they tried to estimate. That such methods lead to statistical problems was also seen by Lawler [26] who discussed the "loop erased SAW". He showed that the procedure of generating walks by SS and then, when an intersection occurs, only throwing away this last loop, leads to a biased sample. Recently he showed [77] that this technique leads to a special case of the Laplacian walk [78] for which it is even not known whether it is in the same universality class as the SAW.

Again a different way is to try to combine various methods. This is done by Rapaport [79]

who combines the dimerization method with the enrichment technique. It is used to calculate the exponent ν and estimate corrections to scaling for $d = 3$ [79] and $d = 2$, 4 [80]. The idea is to construct an enrichment scheme not for single segments, but to use already existing walks as segments to be added. Then the success in generating walks is significantly enhanced due to the high dimerization success rates. However, there might occur a problem. As we saw in the dimerization chapter, in order to obtain an unbiased sample the two parts to be connected have to be taken randomly out of all possible configurations! The way this is done here is that a certain number of medium range SAW's (e.g. 20000 for $N = 60$, $d = 3$ [79]) is used as "segments" for the further generation by enrichment. This source was enlarged by rotating the chains randomly, however, one has to be very careful making sure that the source contains a representative sample of all possible "segments".

2.2. Dynamic methods

While static Monte Carlo methods generate a sequence of statistically independent configurations, dynamic Monte Carlo methods are always based on some stochastic Markov process, where subsequent configurations $\boldsymbol{X}_\nu$ of the system are generated from the previous configuration $\{\boldsymbol{X} \to \boldsymbol{X}' \to \boldsymbol{X}'' \to \cdots\}$ with some transition probability $W(\boldsymbol{X} \to \boldsymbol{X}')$. To a large extent, the choice of the basic move $\boldsymbol{X} \to \boldsymbol{X}'$ is arbitrary various methods as shown in fig. 1.3a–c just differ by the choice of the basic "unit of motion". Also the choice of transition probability $W(\boldsymbol{X} \to \boldsymbol{X}')$ is not unique: we only require the principle of detailed balance with the equilibrium distribution $P_{\text{eq}}(\boldsymbol{X})$,

$$P_{\text{eq}}(\boldsymbol{X}) W(\boldsymbol{X} \to \boldsymbol{X}') = P_{\text{eq}}(\boldsymbol{X}') W(\boldsymbol{X}' \to \boldsymbol{X}). \tag{2.17}$$

In the athermal case (pure SAW problem) each configuration has exactly the same weight, the normalized probability simply is $P_{\text{eq}}(\boldsymbol{X}) = 1/Z_N^{\text{SAW}}$. Then eq. (2.17) says that the probability to select a motion $\boldsymbol{X} \to \boldsymbol{X}'$ must be the same as the probability for the inverse motion, $\boldsymbol{X}' \to \boldsymbol{X}$. One has to be very careful to preserve this symmetry in the actual realization of the algorithm, in particular if one has a choice between several types of move (e.g. fig. 1.3a).

If there is an additional energy $\mathcal{H}(\boldsymbol{X})$ in the problem depending on the configuration $\boldsymbol{X}$, the equilibrium distribution $P_{\text{eq}}(\boldsymbol{X}) = (1/Z) \exp\{-\mathcal{H}(\boldsymbol{X})/k_{\text{B}}T\}$ and hence eq. (2.17) leads to a requirement ($\delta\mathcal{H} \equiv \mathcal{H}(\boldsymbol{X}') - \mathcal{H}(\boldsymbol{X})$ = energy produced by the move)

$$\frac{W(\boldsymbol{X} \to \boldsymbol{X}')}{W(\boldsymbol{X}' \to \boldsymbol{X})} = \exp\{-\delta\mathcal{H}/k_{\text{B}}T\}. \tag{2.18}$$

Following Metropolis et al. [81] we can take the transition probability as for the athermal case (which also results for the model in the limit $T \to \infty$) but multiply it with a factor $\exp\{-\delta\mathcal{H}/k_{\text{B}}T\}$ if $\delta\mathcal{H} > 0$, and leave it unchanged if $\delta\mathcal{H} \leq 0$. Then eq. (2.18) is automatically fulfilled at finite temperature, if it was fulfilled in the athermal case.

In practice, at every step of the algorithm one performs a trial move $\boldsymbol{X} \to \boldsymbol{X}'$. If $W(\boldsymbol{X} \to \boldsymbol{X}')$ is zero (SAW condition being violated), the old configuration is counted once more in the averaging, and the procedure is iterated. If $W(\boldsymbol{X} \to \boldsymbol{X}')$ is unity, the new configuration is

accepted and counted in the averaging. If $0 < W < 1$, we need a (pseudo-) random number z uniformly distributed between zero and one. We compare z with W: if $W \geq z$ we accept the new configuration and count it, while if $W < z$ we reject the trial configuration and again count once more the old configuration.

In the limit where the number of configurations M generated tends to infinity, the states $\boldsymbol{X}$ generated with this procedure are distributed proportional to the equilibrium distribution $P_{\mathrm{eq}}(\boldsymbol{X})$, *provided there is no problem with the ergodicity of the algorithm* (this point will be discussed later). Then the canonical average of any observable $A(\boldsymbol{X})$ is approximated by the simple arithmetic average,

$$\langle A \rangle \approx \bar{A} = \frac{1}{M - M_0} \sum_{\nu = M_0 + 1}^{M} A(\boldsymbol{X}_\nu) = \frac{1}{(t - t_0)} \int_{t_0}^{t} \mathrm{d}t' \, A(t') \tag{2.19}$$

which also can be interpreted as a time average [82] if we associate a (pseudo-) time variable $t' \equiv \nu / \tilde{N}$ with the label ν of successively generated configurations with $t_0 = M_0/\tilde{N}$, $t = M/\tilde{N}$ ($\tilde{N}$ is the total number of monomers in the system, $\tilde{N}$ = (chain length N) $\times$ (number of chains n_c). Since many moves $\boldsymbol{X} \to \boldsymbol{X}'$ involve a motion of a single or a few monomer(s) only, see fig. 1.4a, b, we choose one Monte Carlo step (MCS) per monomer as the time unit). In this interpretation, the Monte Carlo procedure is just interpreted as numerical realization of a Markov process described by a markovian master equation for the probability $P(\boldsymbol{X}, t)$ that a configuration $\boldsymbol{X}$ occurs at time t [82],

$$\frac{\mathrm{d}}{\mathrm{d}t} P(\boldsymbol{X}, t) = - \sum_{\boldsymbol{X}'} W(\boldsymbol{X} \to \boldsymbol{X}') P(\boldsymbol{X}, t) + \sum_{\boldsymbol{X}'} W(\boldsymbol{X}' \to \boldsymbol{X}) P(\boldsymbol{X}', t). \tag{2.20}$$

Obviously, eq. (2.17) suffices that $P_{\mathrm{eq}}(\boldsymbol{X})$ is the steady-state solution of eq. (2.20). If all states are mutually accessible, $P(\boldsymbol{X}, t)$ must relax towards $P_{\mathrm{eq}}(\boldsymbol{X})$ as $t \to \infty$, irrespective of the initial condition.

The dynamic interpretation of the Metropolis [81] Monte Carlo method is useful in two respects:

(i) One can deal with the dynamics of polymeric systems. E.g., one of the basic models of polymer dynamics is the Rouse model [83,12] describing the Brownian motion of a chain in a heat bath. The heat bath is believed to induce stochastically local configuration changes. In a lattice model, this basically amounts to motions of the type considered in fig. 1.4a (for the rigid bond length model) or fig. 1.4d (for the model with fluctuating bond lengths, respectively). It is believed that the Rouse model accounts for the dynamics of not too long real chains in concentrated solutions and melts, and hence there is real interest in studying such models as shown in fig. 1.4a and investigate their dynamic properties. On the other hand, dynamic algorithms as shown in fig. 1.4c ("pivot algorithm") certainly have no correspondence to any real dynamics at all.

(ii) In a dynamic Monte Carlo simulation, the starting configuration usually is not representative for the equilibrium distribution (e.g., one may start with a completely stretched out chain). So the system at the beginning of the simulation needs to be "equilibrated": this is why the first M_0 configurations in eq. (2.19) are omitted from the averaging. One needs to know how large one

must choose M_0 in order to avoid a systematic error due to incomplete equilibration. In addition, one wants to know how many configurations $M - M_0$ kept in the averaging need to be generated in order to reach some given statistical error. For simple sampling where the various states are uncorrelated, the error δA of $\bar{A}$ based on n observations $A_\nu \equiv A(\boldsymbol{X}_\nu)$ is, for $n \gg 1$

$$\langle (\delta A)^2 \rangle \approx \left(\langle A^2 \rangle - \langle A \rangle^2 \right)/n, \tag{2.21}$$

but eq. (2.21) does not hold for the Metropolis importance sampling [81] where subsequent configurations are highly correlated with each other. It turns out that answers to these accuracy questions can be given in terms of dynamic relaxation times $\tau_A^{(n\ell)}$, $\tau_A^{(\ell)}$ of the stochastic model defined by eq. (2.20) [82] (note $t_n = t - t_0$ in eq. (2.19)).

$$\langle (\delta A)^2 \rangle \approx \frac{1}{n} \left[\langle A^2 \rangle - \langle A \rangle^2 \right] \left\{ 1 + 2 \left(\tau_A^{(\ell)} / \delta t \right) \right\}, \quad t_n \equiv n\, \delta t \gg \tau_A^{(\ell)}, \tag{2.22}$$

δt being the time-interval between successive observations used to estimate $\langle A \rangle$,

$$\langle (\delta A)^2 \rangle \text{ as } \langle A \rangle \approx \bar{A} = \sum_{\mu=1}^{n} A_\mu / n, \quad \langle (\delta A)^2 \rangle \approx \overline{(\delta A)^2} = \frac{1}{n} \left(\sum_{\mu=1}^{n} \left(A_\mu - \bar{A} \right) \right)^2, \text{ and}$$

$\tau_A^{(\ell)}$ is defined by the integral of a "relaxation function" $\phi_A^{(\ell)}(t)$:

$$\tau_A^{(\ell)} \equiv \int_0^\infty \phi_A^{(\ell)}(t)\, \mathrm{d}t, \quad \phi_A^{(\ell)}(t) \equiv \frac{\langle A(0) A(t) \rangle - \langle A \rangle^2}{\langle A^2 \rangle - \langle A \rangle^2}. \tag{2.23}$$

Similarly, the approach towards equilibrium is characterized by a nonlinear relaxation function $\phi_A^{(n\ell)}(t)$

$$\phi_A^{(n\ell)}(t) \equiv \left[\langle A(t) \rangle - \langle A(\infty) \rangle \right] / \left[\langle A(0) \rangle - \langle A(\infty) \rangle \right], \quad \tau_A^{(n\ell)} \equiv \int_0^\infty \phi_A^{(n\ell)}(t)\, \mathrm{d}t, \tag{2.24}$$

and the condition that the averaging according to eq. (2.19) includes only well-equilibrated configurations then simply reads

$$t_0 \gg \tau_A^{(n\ell)}. \tag{2.25}$$

Note that eq. (2.25) must hold for all quantities $\{A\}$ that are calculated, and hence it is important to focus on the slowest relaxing quantity, for which $\tau_A^{(n\ell)}$ is largest, if one wishes to estimate the suitable choice of t_0 reliably. This matter of time correlations clearly is a rather important one, since already for single random walk chains the Rouse model [83,12] implies that the single-chain relaxation time τ_N grows with N as

$$\tau_N = \hat{\tau} N^2, \tag{2.26}$$

where $\hat{\tau}$ is of order unity if time is measured in the units of MCS/monomer, and an algorithm as

shown in fig. 1.4a is used. This simple Rouse model describes the dynamics of a single-chain simulation with this algorithm only if excluded volume is neglected (studying the dynamics of simple random walks as done by Verdier and collaborators [84–87] for the dynamics of NRRW's). Understanding the N-dependence of τ_N in the presence of excluded volume interaction is a nontrivial matter for some of the algorithms [88–95], as we shall discuss below.

It should be emphasized that for the dynamic Monte Carlo methods it often is interesting not only to estimate static quantities, as considered in eq. (2.19), but one also wishes to extract dynamic correlation functions (such as $\phi_A^{(\ell)}(t)$, eq. (2.23)) or relaxation times (such as $\tau_A^{(\ell)}$, $\tau_A^{(n\ell)}$, eqs. (2.23), (2.24)) from the Monte Carlo sampling. A discussion of the errors in these quantities due to the finite averaging time is far more subtle [96–98]. Since $\phi_A^{(\ell)}(t)$ involves taking a ratio of two quantities estimated from the same finite sequence of configurations, a systematic error (bias) arises in addition to the statistical error [97]. Another systematic error arises in $\tau_A^{(\ell)}$, $\tau_A^{(n\ell)}$ since the time integration cannot be extended to infinity with the function $\phi_A^{(\ell)}(t)$ obtained from the Monte Carlo sampling: typically $\phi_A^{(\ell)}(t)$ becomes indistinguishable from the "statistical noise" already for times t much smaller than t_n. So either the integration involved must be truncated (which involves an unknown systematic error) or one must try to ascertain the analytic form of the relaxation functions $\phi_A^{(\ell)}(t)$, $\phi_A^{(n\ell)}(t)$ at large times from the Monte Carlo data, in order to be able to carry out the integration at large times analytically. Often the relaxation at large times is exponential

$$\ln \phi_A^{(\ell)}(t) = \text{const} - t/\tau_A^{\max}, \quad t \to \infty, \tag{2.27}$$

and typically $\tau_A^{\max}$ and $\tau_A^{(\ell)}$ are of the same order of magnitude. Then a fit of $\phi_A^{(\ell)}(t)$ in the decade where $0.03 < \phi_A^{(\ell)}(t) < 0.3$ to eq. (2.27) yields an estimate of both $\tau_A^{\max}$ and the constant (sometimes also a fit to a sum of two exponentials is carried out in high precision studies of critical slowing down [99]). In this fit, one usually cannot include the time regime $\phi_A^{(\ell)}(t) > 0.3$, since for $t < t_A^{\max}$ eq. (2.27) does not hold, and the regime where $\phi_A^{(\ell)}(t) < 0.03$, since there often $\phi_A^{(\ell)}(t)$ is not large enough in comparison with the statistical noise. Of course, if there is a broad spectrum of relaxation times which contribute to the relaxation, eq. (2.27) is not useful. It even may happen that $\tau_A^{\max} = \infty$ (i.e., the asymptotic relaxation is weaker than exponential, e.g. a power law or a stretched exponential, for instance); this is suggested [95] to occur for the non-length conserving algorithm of fig. 2.4a [100–102]. Some other algorithms ("chain breaking"), which are either locally (fig. 2.4c) [105] or globally (fig. 2.4b, d) [106,107] not length-conserving, so far have been used for dense multichain arrangements only (subsection 3.3), and their relaxation behavior for single chains is as yet unknown, and thus will not be discussed in the present section at all. Note also that this review emphasizes the various methods, but does not fully discuss the physical significance of the results obtained by these methods: see ref. [103] for a complementary review and ref. [104] for a general discussion of critical dynamics.

2.2.1. Kink-jump methods

In Verdier's original work [84–87] where this method was first introduced only single beads were moved; i.e., in fig. 1.4a only "end-bond" and "kink-jump" but no "crankshaft" motion was allowed. For simple random walks, where both lattice sites and lattice bonds may be multiply occupied by the beads and links of the chain, the simulations were consistent with the Rouse

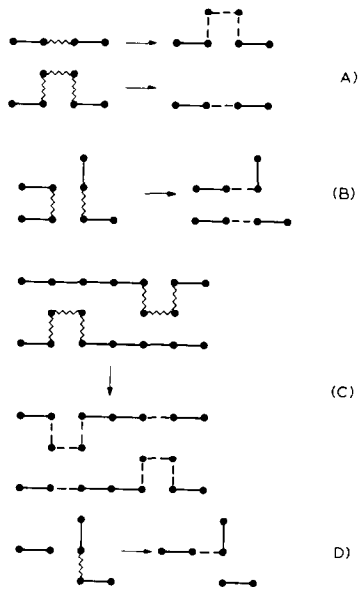

Fig. 2.4. Dynamic Monte Carlo algorithms involving creation or annihilation of pairs of bonds [100–102], case A; or exchange between pairs of parallel bonds which reorient to form a different connection between the two parts of the chain (or two different chains, respectively) [106,107], case B; exchange between crankshaft configurations between two different parts of a chain (or two different chains, respectively [105], case C; rotation of a bond to form a different connection between two parts of a chain (or two different chains, respectively) [106,107], case D.

model [83,12], as far as the long-time properties are concerned. In fact, for the freely jointed chain in the continuum, one can prove exactly [109,108,12] this equivalence between the kind-jump model and the Rouse model. In the presence of excluded volume interaction, the situation is radically different: Verdier [85] suggested that now $\tau_N \propto N^3$. This result at first sight is very surprising, as can be seen from the following heuristic argument [95,3]: as a result of any local motion of beads in a chain, we expect that the center of gravity moves a distance of the order of $\boldsymbol{a}/N$, where $\boldsymbol{a}$ is a vector connecting two nearest neighbor sites on the lattice, and whose orientation is random. These random displacements add up diffusively, and thus after $\tau_N N$ such motions a meansquare displacement of the order of the end-to-end distance square is reached, $(\boldsymbol{a}/N)^2 \tau_N N = \langle R^2 \rangle = N^{2\nu}$. This estimate thus implies that the slowest modes involve long-distance properties of the order of the chain linear dimension; the chain configuration hence should be fully relaxed, when the center of gravity has travelled a distance of the order of $\sqrt{\langle R^2 \rangle}$. This "dynamic scaling" [104] argument hence implies that the diffusion constant of the chain scales with chain length as

$$D_N \propto N^{-1}, \tag{2.28}$$

irrespective of excluded volume restrictions and that the relaxation time scales as

$$\tau_N \propto N^{1+2\nu}. \tag{2.29}$$

For the random walk ($\nu = 1/2$) this indeed reduces to eq. (2.26); but for the SAW in $d = 3$ where $\nu \approx 0.59$ the exponent $1 + 2\nu \approx 2.2$ is much less than 3 as found by Verdier [85]. This large exponent then was attributed [88,89] to the fact that in the presence of exclude volume S-shaped configurations (built up by two successive "crankshafts" in a plane) could only relax by kink-jumps if one of the kinks has diffused towards the chain ends. Hilhorst and Deutch [88] suggested a quicker relaxation should occur if one allows crankshaft motions (fig. 1.4a). It turned out that restricting those crankshaft motions to a plane one still finds $\tau_N \propto N^3$ [90–92] leading to a reptation-like motion [93]. The interpretation of this finding is that one still only interchanges (next-nearest) bond vectors by this algorithm, just as the one-bead kink-jump motion (fig. 1.4a) interchanges nearest-neighbor bond vectors along the chain, but new bond vectors occur only by diffusing into the chain from the chain ends, where they are created by the end-bond motion. It hence is crucial to include the out-of-plane crankshaft rotation [110] to create new bond vectors (in two dimensions, one hence cannot apply this algorithm at all but rather has to use the algorithm shown in fig. 1.4d if one wishes to simulate Rouse dynamics, while for static properties the algorithms of fig. 1.4b, c are applicable). Note that in off-lattice simulations with excluded volume (the "pearl-necklace model") the kink-jump method does generate new bond vectors in three dimensions, and hence the result of eq. (2.29) is in fact consistent with the simulation [111].

Another criticism raised with respect to all local length-conserving algorithms (fig. 1.4a is an example which could be generalized by motions involving 4, 5,... neighboring bonds at a time, of course) is their lack of ergodicity [112–114]. One can identify local dense configurations or configurations with "knots" which cannot relax at all by the motions allowed in the algorithm. In $d = 2$, a configuration with $N = 16$ can be drawn on the square lattice which is completely frozen, if the algorithm of fig. 1.4a or that of fig. 1.4b is applied; in $d = 3$ a knot which cannot relax by the algorithm of fig. 1.4a occurs on the sc lattice already with $N = 19$ beads [112].

Thus by the kink-jump method and its variants one does not sample the full phase space, but only an "ergodic subclass" of the configuration space from which these "forbidden configurations" are omitted: since these configurations cannot relax, the detailed balance principle also implies that they are not reached in the course of the simulation. Although this lack of ergodicity is a serious problem in principle, its practical consequences seem to be irrelevant: for the chain lengths and lattice for which the "kink-jump"-method can be applied, the systematic error (due to the failure of including the forbidden configurations) seems to be smaller than the statistical error. This is to be expected, since the total number of configurations grows exponentially fast with N {cf. eq. (1.2)}, and so does the total number of accessible configurations. Even though for large enough N almost every chain configuration occurring in the full phase space has groups of bonds which are locked in, the fraction of bonds which are locked in is small for $N \to \infty$ for almost every chain configuration. If we then replace in such a chain configuration every group of locked-in bonds by a group of less bonds which is mobile, we transform the chain from a chainlength N to a chainlength $N' = N - \Delta N$ with $\Delta N/N$ small, but identical long-wavelength properties ($\langle R^2 \rangle$, $\langle R^2_{\text{gyr}} \rangle$ etc. are nearly identical for both chains). Since for almost every locked-in chain a non-locked-in chain with nearly identical long-wavelength properties can be found, we expect that the ensembe of chains which are not locked-in does in fact generate results for $\langle R^2 \rangle$, $\langle R^2_{\text{gyr}} \rangle$ etc. which are representative for the full ensemble.

In addition, all comparisons between numerical results obtained with this algorithm and with static algorithms (subsection 2.1) show that the results do not suffer from ergodicity problems.

Values for $\langle R^2 \rangle$ on the sc lattice are tabulated by Verdier [85] for $N = 8$, 16, 32 and 64 and by Kranbuehl and Verdier [90] for $N = 9$, 15, 33 and 63; within the statistical uncertainties quoted, these numbers do agree with the corresponding static results. Similar agreement was noted by Kremer et al. [21] in work on the tetrahedral lattice.

The kink-jump method is most useful when one is interested in time-dependent properties of the chains, since this algorithm rather closely corresponds to the Rouse model, as has been demonstrated by a number of studies [84,115–119]. But most valuable is this algorithm for the simulation of many-chain systems, see subsection 3.1.

One must be very careful in the precise choice of the algorithm in order to obtain valid results [116]. In our view, the crucial point is that new bond vectors can be generated not only on the ends, so that the algorithm would be able to equilibrate also ring polymers, and that one does not introduce an artificial bias into the choice of local motions. For instance, in ref. [120] a 90°-crankshaft motion on the sc lattice is tried and whenever it is not possible a simple one-bead kink-jump motion is tried instead. Although $\tau_N \propto N^{2.13}$ is found in reasonable agreement with eq. (2.29), it is not clear that this algorithm faithfully represents the Rouse model for intermediate wavelength of the modes. In refs. [90,121] both one- and two-bead motions are tried at random, but the two-bead motions involve interchanges of bond vectors only. Then it is not too surprising that the relaxation found is slower than expected from eq. (2.29).

2.2.2. The "Slithering Snake" ("Reptation") Algorithm

The generation of SAW configurations by the "Slithering Snake" algorithm was originally suggested by Kron [122] and by Wall and Mandel [123]: one randomly selects one of the ends of the chain and removes the end bond there, and at the same time at the other end of the chain one adds a bond in a random orientation. Of course, this trial move again is carried out only if it does not violate excluded volume restrictions (if interaction energies are present, the move is carried out only according to the transition probability W, as discussed after eq. (2.18)).

Clearly, this algorithm is relatively simple, and although it is not a realistic description of chain motions on a local scale (i.e., for distances smaller than the radius of the coil), it leads to rather quick equilibration of the coil, the relaxation time being smaller than according to the Rouse model (eq. (2.29)). Qualitatively, one can argue that the center of mass vector moves a distance of $|\boldsymbol{R}|/N$ at each attempted move, and again requesting that during the time τ_N ($\tau_N N$ attempted moves) the mean square displacement is of the order of $\langle R^2 \rangle$ we find $(\langle R^2 \rangle / N^2)\tau_N N = \langle R^2 \rangle$, i.e. $\tau_N \propto N$. While some investigators claim that this is what they observe [95,98] work employing a dynamic Monte Carlo renormalization group [124] finds a slightly larger exponent, $\tau_N \propto N^{1.02}$ ($d = 3$) and $\tau_N \propto N^{1.15}$ ($d = 2$). Note that in ref. [124] the time unit for the slithering snake mechanism was defined 1 elementary move rather than 1 elementary move per bond, so the dynamic exponent z defined from $\tau_N \propto \langle R^2 \rangle^{z/2}$ in ref. [124] exceeds the value which it has for the slithering snake model in our notation by a factor $[1 + 1/(z\nu)]$. On the other hand, for the Rouse model ref. [124] uses one move per bond as time unit, and then the dynamic exponent has its standard value $z^{\text{Rouse}} = 2 + 1/\nu$. If the results of ref. [124] are numerically reliable, the implication is that the excluded-volume interaction leads to nontrivial longlived dynamic correlations, so that the above simple estimate $\tau_N \propto N$ based on random walk ideas is not valid. This point deserves further investigation.

Also for this algorithm, it is clear that it cannot be strictly ergodic: if all nearest-neighbor sites

of the two chain ends are occupied, no motion whatsoever is possible. Again these locked-in configurations cannot be reached from the "ergodic subclass" to which this algorithm is restricted. It is a general feeling that for the study of athermal SAW's the systematic errors are negligible in comparison with the statistical errors (e.g., in ref. [124] where $N = 32$ and $N = 64$ was studied, the quoted relative statistical error is roughly one percent). Probably this non-ergodicity problem would become serious if the method were applied to studies of the collapse transition of single chains, where rather dense configurations get a high statistical weight. The main application, however, of this algorithm rather is the simulation of multi-chain systems (subsection 3.1) and then the algorithm seems to be rather efficient. One can of course get rid of the ergodicity problems of this algorithm (as well as of the kink-jump algorithm) by working with a repulsive potential of finite strength for configurations where chains intersect, rather than with the strict excluded volume condition (corresponding to an infinitely high repulsive potential). From the universality principle of critical exponents [3,125] it follows that exponents such as γ, ν, z do not depend on the strength of the excluded volume potential, i.e., are the same for finite and for infinite strength. However, these universal exponents in principle apply to the limit $N \to \infty$ only: the weaker the strength of the excluded volume potential is, the larger values of N are actually needed to reach this asymptotic regime, while for the strict SAW model the asymptotic regime extends to fairly small values of N, since corrections to scaling terms have numerically small effect only. For $N < 10^2$, to which methods discussed in this and the previous section typically are restricted, the variation of the strength of the excluded volume interaction [121] leads to a smooth variation of "effective exponents" and the true asymptotic behavior is rather hard to ascertain.

The present method is not a realistic model for polymer dynamics on length scales shorter than the coil size, but it is much quicker than the kink-jump algorithms. For multi-chain systems, one often is interested in dynamical properties on long wavelengths only (e.g. the simulation of the dynamics of phase separation in polymer mixtures [126]): then the present method is useful even for dynamic properties, if the N-dependence of characteristic times is scaled out suitably.

2.2.3. The "Wiggle" ("Pivot") Algorithm

There we are concerned with the method schematically illustrated in fig. 1.4c: Starting from some configuration of a SAW, we randomly select one site of the walk (which can be anywhere on the walk). A symmetry operation of the lattice (rotation or reflection) is applied to the part of the walk subsequent to the selected site, using this site as the origin. The choice of this symmetry operation is at random. The resulting walk is accepted if it is self-avoiding; otherwise it is rejected and the old walk is counted once again.

This algorithm was first invented in 1967 [127] and first found little attention [128], but gained more popularity [129,130,60] when it was reinvented recently [129,130]. In a thorough recent paper, Madras and Sokal [60] analyze this algorithm analytically for the ordinary random walk case, and prove that for the SAW this algorithm is ergodic. They suggest that the fraction f of accepted trial configurations decreases as a power-law with increasing chain length N, $f \propto N^{-p}$, and find that the exponent p is quite small ($p \approx 0.2$ for two dimensions). Therefore the autocorrelation time of the walk behaves as $\tau \propto N^p$ and hence increases distinctly slower with N than all the other algorithms described so far. Of course, the present algorithm has no relation any more to any actual motions of a polymer chain in a solvent, but nevertheless seems to be

very useful to obtain highly precise estimates for the exponent ν ($\nu = 0.7496 \pm 0.0007$ ($d = 2$) and $\nu = 0.592 \pm 0.003$ ($d = 3$) [60] using SAW's of length $200 \leqslant N \leqslant 10^4$ ($d = 2$) and $200 \leqslant N \leqslant 3000$ ($d = 3$)). Although this algorithm is extremely efficient (with N such elementary motions one generates an essentially new configuration), one has to be careful in "equilibrating" the system after the start in some arbitrary initial configuration: At least of the order $10N^2$ elementary motions are needed for "thermalization", since the largest relaxation time of this algorithm scales differently from the "average" autocorrelation time τ. This problem is avoided, however, if one uses configurations constructed by a suitable static method (e.g. dimerization [57]) as initial configurations.

While this algorithm clearly is very useful for studying long isolated chains, it is probably not suited for a generalization to simulate dense multichain systems.

2.2.4. Bond fluctuation method

A different approach was used for the bond fluctuation method [131] of Carmesin and Kremer. The aim was to give an algorithm which allows for an analysis of dynamic properties in all spatial dimensions and which is ergodic. Since a dynamic interpretation is required, the number of bonds has to be conserved and the motion must be constructed out of local jumps. The local jumps had to be set up in a way, that new bond vectors are created with such a jump. No standard 2-d algorithm can be used to extract information on the dynamics of chains. Here we describe this method for $d = 2$, since this is the most crucial case. The chains are implemented on a square lattice (lattice constant 1). Each monomer occupies $n_m = 4$ lattice sites of a unit cell $(2 - d)$. Each lattice site can only be part of one monomer (SAW condition). The bond length ℓ has to be smaller than $\ell_{max} = \sqrt{16}$. To move the chain a monomer is selected at random. Then the monomer tries (at random) to jump one lattice constant into one of the 4 lattice directions. If the move complies with the above restrictions it is accepted, otherwise one has to select a new monomer. Of course, other suitable choices of n_m, ℓ_{max} are also possible (e.g., for polymer mixtures one might consider two types of chains with different choices of n_m, ℓ_{max} on the lattice).

This is illustrated in fig. 1.4d. Clearly this approach fulfills the detailed balance condition. A similar approach in continuum was used by Kantor et al. [132] for the simulation of tethered surfaces. For the NRRW this model displays the pure Rouse behavior [131]. For the SAW with this approach the SAW influence on the mean square displacement of the individual monomers [12,133] was demonstrated. Since the monomers only move a short distance compared to a bond length at each jump the prefactor for the time needed to obtain static properties is larger than for standard lattice models. Since the persistence length is smaller, however, this is somewhat compensated. Also this is the only MC algorithm so far which allows for the dynamic simulation of branched polymers. Although ergodicity is not a problem for the simulations of individual chains, for the application to very dense systems this might be important. Fig. 2.5 displays how the bond fluctuation algorithm can get out of a typical blocking configuration as they were discussed by Madras and Sokal [112]. Therefore, the main applications of this approach will be for branched and/or dense polymer systems [134]. Note that in all lattice models of polymers a bond of the lattice chain is not thought to correspond to a chemical C–C bond (fig. 1.1) but rather to a group of successive chemicals bonds; thus a fluctuation in length of these effective bonds is physically reasonable.

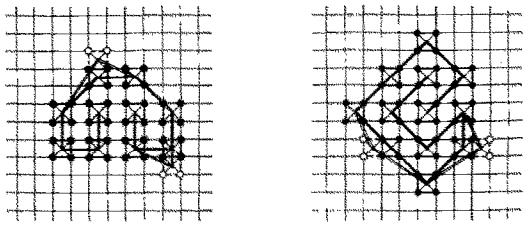

Fig. 2.5. Illustration how the bond fluctuation method leaves a configuration which for standard kink-jump methods is blocked (from ref. [131]).

2.3. Grand canonical methods

The grand canonical MC methods for single chains allow the addition and in some cases the annihilation of bonds by a random procedure. The acceptance of these attempts is governed by the chemical potential μ leading to an average chainlength $\langle N \rangle$. Two of these methods are based on a successive replacement/deformation of the chains. Contrary to most static methods the configurations are highly correlated. This, besides the discussion of the technical aspects, has to be analyzed similar to the other dynamic methods (subsection 2.2). There are three single chain grand canonical methods in use. One originates in a Monte Carlo sampling of generating functions for large cell renormalization. This is a static method and was first used by Redner and Reynolds [135]. The two other methods are dynamical in a sense, that they allow a deformation and/or growth/decrease of a given conformation. Beretti and Sokal [98] propose a method where such changes are confined to an end of the walk. Based on a more general method of Berg and Förster [100] Carvalho and Caracciolo [101,102] give an algorithm where such changes can occur anywhere in the chain.

First lets turn to the Redner Reynolds [135] method. Their idea came out of an enumeration problem of a real space renormalization group (RG). Since they wanted to perform a large cell RG calculation, they had to find a substitute for the enumeration of all spanning walks. They tried to sample the generation function by Monte Carlo. To explain it we discuss the generation of SAW's starting at a given lattice point. The generating function $\Gamma(p)$ then is:

$$\Gamma(p) = \sum_N Z_N p^N. \tag{2.30}$$

Note that $\Gamma(p)$ is nothing else as the grand canonical partition function, if we interpret p as the fugacity per bond. Thus they call their approach constant fugacity Monte Carlo. Note that there are conceptual similarities to the enrichment approach. Starting with an enumeration routine each step now only is continued with the probability p (< 1). By this they sample $\Gamma(p)$. For p approaching p_c ($= 1/q_{\text{eff}}$) $\Gamma(p)$ diverges as $(p - p_c)^{-\gamma}$. For magnets that is just the divergence of the susceptibility at the critical point. For $p < p_c$ $\Gamma(p)$ remains finite leading to a finite average polymer length $\langle N \rangle$. Similar the end to end distance is given by

$$\begin{aligned} \xi^2(p) = \sum_{N,r} r^2 C_{N,r} p^N / \Gamma(p) \quad &\propto (p - p_c)^{-2\nu}, \\ &\propto \langle N \rangle^{2\nu}, \end{aligned} \tag{2.31}$$

$C_{N,r}$ now is the number of all walks with N bonds and an end to end distance r.

Note that this approach starts from the generation of the partition function, while the other methods start from the collection of properties of single chains. This method then was generalized to lattice animals and branched objects by Dhar and Lam [136]. The method was also used to calculate winding angles of 2-d SAW's [137] as well as e.g. the problem of the diverging persistence length in 2d [138,139].

The above mentioned other two methods [98,100–102] go back to the principle of modifying a single chain. While the first method [135] at each "run" produces a statistical estimate of $\Gamma(p)$, which is uncorrelated to the previous one, one here has to take care of the relaxation rate of the object under consideration. First let us discuss the method of Beretti and Sokal. They also start from the grand canonical partition function of eq. (2.30). They constructed a dynamic MC algorithm. The "elementary moves" are to attempt to add a new bond with probability P, where each of the q lattice directions are equally probable. This leaves the probability $P(\Delta N = -1) = 1 - qP(\Delta N = +1)$ for the annihilation of a bond. The absolut value of the probability $P(\Delta N = +1)$ then is governed by the fugacity per bond β. If the new bond violates the SAW-condition, the attempt is of course rejected. The normalization of the probabilities then gives

$$P(\Delta N = +1 \text{ attempt}) = q\beta/(1 + q\beta)$$

leaving a probability

$$P(\Delta N = -1) = 1/(1 + q\beta) \tag{2.32}$$

for the annihilation of a bond. This relation satisfies the probability normalization. Note that $P(\Delta N = +1$ attempt) is the sum over all lattice directions leaving $\beta/(1 + q\beta)$ for a specific step. This method, as shown by the authors, satisfies the detailed balance condition and is ergodic, in the sense that it reaches any possible SAW configuration. The authors perform a very thorough statistical analysis of the properties of their algorithm. They argue that the relaxation time between two independent configurations τ is of the order of $\langle N \rangle^2$, measured in elementary computer operations like the attempt of adding a bond. They argue that one needs a time $\tau \propto \langle N^2 \rangle$ to delete a chain completely and again a time $\tau \propto \langle N^2 \rangle$ to build it up again. Note that typically the time unit is one operation per bond. To compare the time here to the ones quoted in subsection 2.2 one has to divide τ by $\langle N \rangle$, giving $\tau \propto \langle N \rangle$. However, it is not clear whether this time due to the SAW constraints follows a slightly higher exponent or not. Studies using the slithering snake algorithm, which they claim shows the same relaxation behavior, find a enhanced relaxation time (see subsection 2.3). The third [100–102] algorithm allows also for changes in the middle of the chain. For illustration all three algorithms are compared in fig. 2.4. Carvalho and Carraciolo [101] use the same statistical ensemble as ref. [98]. However, the modification of the chain is *not* confined to the end of the chain. First let us explain the case of fixed end points. Then the procedure is as follows. The algorithm as it is given is confined to a hypercubic lattice, but generalizations are straightforward. Fig. 2.4a illustrates this. A bond is selected at random. Then it is displaced at random by one lattice unit to one of the $2(d-1)$ directions orthogonal to the bond. If this attempt to move violates the SAW condition it is of course rejected. If it complies with the SAW condition there are three possibilities either $\Delta N = +2$ or -2 or $\Delta N = 0$. In order to satisfy the detailed balance condition the probabilities

$p(\Delta N)$, chosen independent of the step and the directions have to follow $p(\Delta N)/p(-\Delta N) = \beta^{\Delta N}$. Thus here $\beta^{1/2}$ is the fugacity per bond. The philosophy here is coming from sampling correlation paths between two points for the n-vector model with $n \to 0$. If also the ends are allowed to move, one has to incorporate slight modifications. For the ends this leads to the same probabilities as in the Beretti–Sokal method [98]. This method was used in a rather general study of ϕ^4 field theories [102]. Again also here one has to take care of the relaxation time of the algorithm, since the subsequent conformations are highly correlated. In a recent comparative study [95], Caracciolo and Sokal investigate the relaxation properties of a large group of dynamic MC algorithms for SAW's. Note that we here use the time definition of subsection 2.2. They argue that in general kink jump algorithm should display a relaxation time τ with $\tau \propto N^{1+2\nu}$, with $\nu = 1/2$ for NRRW's and $\nu = 0.75$ ($d = 2$), 0.59 ($d = 3$). The time again is measured in units of e.g. attempted moves per bond as done in subsection 2.2 (Note the difference in the measure of the time unit here and in ref. [95].) The present algorithm they study for $d = 2$ for the NRRW and the SAW. They find $\tau \propto N^{1.0 \pm 0.5}$ (NRRW), $\tau \propto N^{1.0 \pm 0.5}$ (SAW). This indicates that this method is slightly slower than the Beretti–Sokal method [98] and slightly faster than standard dynamic methods [95] see also subsection 2.2). However, the error bars are fairly large and the chains considered were relatively short ($\langle N \rangle \leqslant 65$).

Although these grand canonical methods are very interesting and probably have a potentially large area of application, they are not widely used yet.

2.4. Comparison and application

The present paragraph tries to illustrate several ways of analyzing data and in the course of this to give hints for applications. There exist some comparative studies [70,95], however, they are confined to rather special cases. The various methods are too different in order to easily devise the one and only useful method. It is also beyond the scope of the present paper to perform a deep statistical analysis of all the methods, although this rarely has been done yet. The few exceptions are already mentioned. In the previous chapters we explained the specific strength or weakness of the various methods. We here now want to compare the methods in view of their possible applications. The way most algorithms are discussed up to now is with respect to properties of pure SAW's. However, quite often the interesting polymer problems are not the ones which can be analyzed by the bare models themselves. By comparing various approaches with respect to typical linear chain applications, we also discuss some aspects of how to extract physical quantities. Very interesting other classes of systems are discussed in the following two chapters, namely branched polymers and polymers in confined geometries.

In addition to the methods here discussed, there exists a huge class of models which were proposed for special applications (Fractals, True SAW, SA Trail) [140,141]. They are from a physical point of view certainly of high interest, since they at least in some cases share the same universality class as polymers. For such models, however, the direct correspondence to polymers in general is not clear. Therefore we here confine ourselves to methods which are suitable to simulate equilibrium properties and allow the way of mapping onto "real polymers" explained in the introduction.

2.4.1. When which method? Linear chains

To answer this question ahead of an investigation is very difficult. Most of the methods were used and discussed for properties of pure SAW's without any further interaction. Let us first consider this case. There is one trivial decision. If one wants to investigate dynamic properties on internal length scales one is confined to the algorithms of subsections 2.2.1 and 2.2.4. These are the only ways of getting direct information on dynamical properties. Then one has to pay the price of a "realistically slow" kinetics. Information on static properties then is produced as byproducts. However, there is also a way of getting some dynamic information out of static properties. Zimm [142] was the first who used static properties to deduce dynamic information like the initial decay of the structure function. First now let us turn to the end to end distance $\langle R^2(N)\rangle \propto N^{2\nu}$. Since the relative fluctuation of $R^2(N)$ does not vanish with large N one needs either relatively accurate data for many chainlengths, extending over several decades or one needs very precise data of short chains in order to extrapolate. One way e.g. would be to generate a sample of many chainlengths by the pivot algorithm. Since one can run a simulation only for one chainlength, this needs many independent runs. The same holds for a grand canonical simulation, where one has to vary the fugacity. One the other hand, one can use SS or biased sampling or the dimerization and/or enrichment. There one gets data for a huge number of chainlengths within one run. This may then be more economic than the use of the previously mentioned methods. However, the problem one encounters is that the data of different chainlengths are correlated. This can be clearly seen from the "correlated scatter" of data, making precise error estimates rather difficult. Fig. 2.2a gives an especially clear example for illustration. Another problem occurs if one wants to analyze corrections to scaling. For $d = 2$, 3 one expects [143,144]

$$R^2(N) = AN^{2\nu}(1 + BN^{-\Delta} + \cdots), \tag{2.33}$$

while for $d = 4$

$$R^2(N) = AN^1(\ln^{\Delta} N + \cdots), \tag{2.34}$$

where Δ is some "correction to scaling-exponent". This suggests that for $d = 2$, 3 short chains but very precisely sampled are the best since the corrections have the form of a power law with a negative exponent. This can be done either directly by series enumeration [144] and/or Monte Carlo ratio methods ("Monte Carlo series expansion") [145]. The case $d = 4$, however, needs very long chains in order to identify the ln correction as the dominant one [146,147]. Rapaport uses a combination of dimerization and enrichment to obtain information on corrections to scaling [146]. A different way of finding ν is either by the use of the scattering function or by the concept of local fractal dimensionality (LFD) [148], which can also be used to estimate corrections to scaling [146]. For the scattering function the fractal scattering law [149] gives

$$S(k) \propto k^{-1/\nu} \tag{2.35}$$

for $2\pi/\ell \gg k \gg 2\pi/\langle R^2\rangle^{1/2}$ where ℓ is the bond length. This yields already for very short chains reasonable results. The LFD concept uses similar to the scattering function all internal

distances. Both make use of the self similar structure of the chains. Assuming that $R^2 \propto N^{2\nu}$ also should hold for internal distances Havlin and Ben Avraham define the LFD as [148,150]

$$D_{N_0}(N) = \ln\frac{N+1}{N} / \ln\left(\frac{\langle R^2(N+1)\rangle_{N_0}}{\langle R^2(N)\rangle_{N_0}}\right) \tag{2.36}$$

with $D_{N_0\to\infty}(N\to\infty) = \nu^{-1}$. N_0 is the length of the chain and with $N < N_0$ $\langle R^2(N)\rangle_{N_0}$ means the average over all partial N step chains. This method was used for dimensions 2–5 [148] and for data generated by a large variety of methods [70]. However, in order to find the exponent γ probably the dimerization is the most direct way, see eq. (2.15). In order to find q_{eff}, the connectivity, again simple sampling or enumeration still may be the most appropriate procedure. Using this, the exponent γ can be found by simple ratio methods. Nevertheless, in order to judge the quality of numerical data the authors should give the number of statistically independent chains as well as the way of calculating the errors. A very detailed and elaborate way of error estimates is given by Beretti and Sokal [98] on the basis of probability theory. Other than direct approaches are of course the use of real space Monte Carlo renormalization. For a discussion of these ideas we refer to the book of Burkhardt and van Leeuwen [150]. Real space Monte Carlo renormalization of off-lattice chains has also been proposed [151].

So far we discussed the case of the pure SAW. From the view of polymer physics this is a standard case, but not the one which is in the center of present research interests.

The pure SAW corresponds to the so-called good solvent. Many experimentally interesting objects are in θ-solvents. Thus the nature of the θ transition is of special interest. For $d = 3$ most of the studies used either SS or biased sampling methods (see subsection 2.1). These methods have the advantage of giving the free energy of the chain directly. For reasons discussed in subsection 2.1.2 all static methods, besides the biased sampling approach, share the problem of sampling the relevant part of the distribution function. Another way out was proposed by Meirovitch [54]. He wants to introduce a temperature in his scanning method in order to account for the attraction of the monomers. A different way would be to use a dynamic method or a grand-canonical one in connection with a Metropolis sampling. The disadvantage here is that results are only produced for one temperature and one chain length. For $d = 3$ we think that the biased sampling method is the genuine approach to study the collapse transition. For the $d = 2$ collapse transition the situation is especially difficult. Baumgärtner [152] used the slithering snake algorithm on the square lattice, while Birshtein et al. use a biased sampling with the restriction of infinite growth [42]. However, the results are quite contradictory.

Recently two special classes of linear polymers were investigated. Block copolymers were analyzed by the biased sampling method [153]. There is clearly much more work needed. The other class are ring polymers [154]. They used a dimerization approach to construct rings. Ten Brinke and Hadziiaonnou [155] used a modified pivot algorithm for RW rings. Wiegel et al. [156] also studied RW rings, but in the continuum. Up to now there is no detailed study on the properties of SAW-ring polymers.

Dilute and semidilute solutions up to now have been rarely investigated. Öttinger used the scanning method to calculate the osmotic pressure of a semidilute polymer solution [52]. Most attempts for many chain systems aim to study polymer melts (see subsection 3).

2.4.2. Confined geometries

Many polymer problems are governed by strongly confined geometries. Here we especially think of chains near surfaces or interfaces or in tubes [133]. Especially if one seeks for the adsorption transition the use of specialized biased sampling methods is useful. Clark, Lal and coworkers [157] used a kind of kink jump algorithm to study the properties of chains on a diamond lattice near surfaces and in slits. Wall and Mandel [158] used the slithering snake method to study properties of chains near surfaces while Webman et al. [159] used the slithering snake method in continuum to study the crossover from three-dimensional behavior to two-dimensional behavior by varying the width of a slit. The first pioneering Monte Carlo study of the adsorption transition of SAW's was performed by McCrackin [160]. He used the biased sampling method. However, this encounters for large chains the typical problems discussed in subsection 2.1.2. Later investigations used for this problem [46] and related ones like the adsorption at a penetrable interface [47] or the adsorption of a θ-chain [161] a more specialized approach. Fig. 2.6 gives an example of the scaling of the energy for adsorbed chain. The data were obtained by using a soft bias for the penetration of the interface layer, which made the interface either slightly attractive or repulsive. They use a (soft) bias only for the surface. This makes that, similar to the θ-problem, the generically sampled distribution is the one approximately at the transition temperature. Fig. 2.7 shows a test of the validity of various soft biases for chains near a surface. Cosgrove et al. [162] and Meirovitch [53] used the scanning method for chains confined

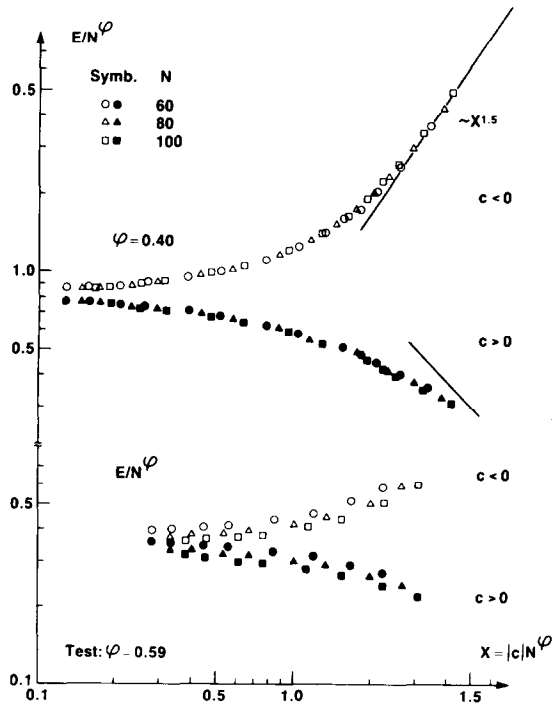

Fig. 2.6. Scaling plot for the number of adsorbed monomers E divided by N^{φ}, with φ the crossover exponent vs the scaling argument $|C|N^{\varphi}$ for two choices of φ proposed in the literature. The chain adsorbes at penetrable interface. The data were obtained using as soft interface bias [47].

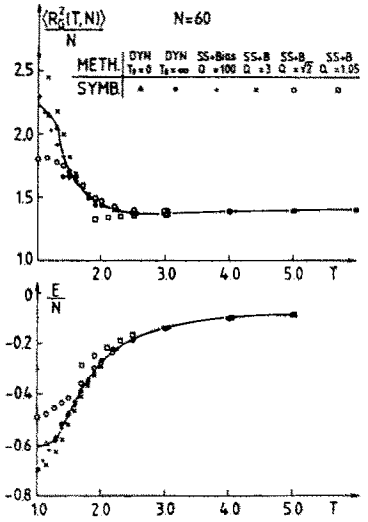

Fig. 2.7. Comparison of surface bias data with data obtained by kink-jump method for the adsorption of polymers at a surface. Taken from ref. [46].

to a box in order to calculate the entropy of such objects. Recently the scanning method was also used to study the adsorption of a single chain [163]. A completely different problem occurs for chains confined to disordered lattices. One can here think of polymers in porous media. It seems to be that a suitable approach for strongly diluted lattices is the slithering snake method [164]. Baumgärtner and Muthukumar [165] studied chains in porous media in continuum. To analyze the dynamics they used the kink jump method while for static properties they apply standard simple sampling.

Additional interesting problems arise for many chain systems in confined geometries, see e.g. [196] (see section 3). To us it seems that a combination of specialized biased sampling methods with other approaches like dimerization might lead to many new and interesting results.

2.4.3. Branched rather than linear chains

With the fast development of the preparative chemistry, branched polymers like stars or combs etc. became experimentally more relevant. First theoretical attempts were made 1949 [166]. But besides the pioneering investigation of Mazur and McCrackin [167,168] who used the biased sampling method for stars and comb polymers, only recently simulations came up to study such systems. We here do not study all the models and literature which occur in the course of investigation of gelation processes. There exist excellent reviews on the subject [141,169] as well as rather complete conference proceedings of recent developments [142]. Besides this area of investigation most authors deal with star polymers. Mazur and Mc Crackin already performed a first analysis of the collapse transition. Kolinski and Sikorksi used the diamond lattice to perform a similar analysis [170,171] in both cases. Both investigations, however, did not take into account a scaling analysis. Theoretically now the question of the form of $\gamma(f)$ is one of the most discussed ones. Miyake and Freed [172] calculated ($d = 3$) $\gamma(f)$ by direct renormalization. While Ohno gets a different result using the lattice magnetic analogy [173], Whittington and coworkers [174] used the biased sampling approach to investigate stars and combs and to calculate $\gamma(f)$

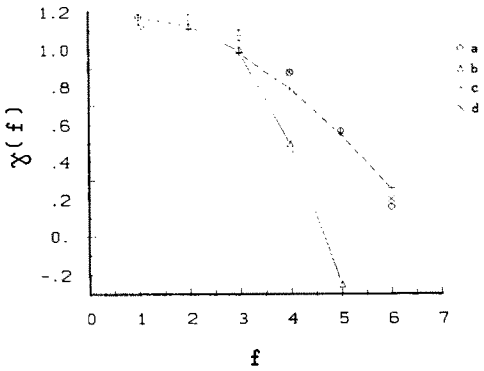

Fig. 2.8. Data for the exponent $\gamma(f)$ for f-arm stars. The data (c) [173] and (b) [172] are taken from different analytic predictions. The indicated lines are guides to the eye. The numerical data are obtained by (a) [66] the modified dimerization method and (d) [175] by biased sampling. Note that the error bars for (a) are smaller than the symbol size, while ranging from 0.03 to 0.05 for (b). The figure is taken from ref. [66].

[175]. They also looked at the overall dimensions of stars as well as combs. However, the use of such biased sampling methods restricts them to rather modest arm lengths. A way out of this problem is given by a recent investigation on the fcc lattice [66]. There the dimerization in the modification of Batoulis [65] was used to construct the arms. Then the dimerization was also used to put together the star polymers. By this the systems dealt with could be made larger and the accuracy of the results increased significantly. Fig. 2.8 gives a comparison of the $\gamma(f)$ calculations of refs. [66,172,173,175]. For other quantities, besides γ, it probably would also be useful to use a kind of pivot algorithm. However, since the center is especially fixed by all the arms one has to check carefully the relaxation time. Typically lattices confine to a relatively small number of arms. To overcome this one either has to go to continuous structures [176] or one has to modify the lattice structure of the systems. Kolinski and Sikorski [170,171] use a diamond lattice and grow the stars in the center out of little trees. A different approach was used by Barrett and Tremain [73]. They use a simple cubic lattice but allow for bonds only connections which give a bond length of $\sqrt{5}$. Their steps look like the jumps of the knight in chess. By this they go up to $f = 24$ arms.

Freire et al. [177] as well as Zimm [178] use a continuum method to calculate hydrodynamic properties. More difficult becomes the analysis of such systems, if one is interested in dynamic properties. Here standard kink jump methods are not very useful. There the crosslink is not allowed to move at all. Evans [179] used simple RW arms in an early study of chains in an entangled environment. This of course yields only results on a very specialized model and the applicability of the data is rather limited. One could of course argue that the shape relaxation may be fast compared to the overall motion. Indeed this was seen for stars with many ($f \geq 20$) arms [175], but for an understanding of smaller branched structures such as stars, combs, microgels or rubber the mobility of the crosslinks is essential. The only way out here is to use Brownian or Molecular dynamics methods which work in continuum or to make use of a bond fluctuation method [131].

To summarize, the Monte Carlo investigation of branched polymers seems to be at its very beginning and may yield many interesting and important results in the near future.

3. Simulation of many-chain systems

Simulation of model systems containing many polymer chains can address a wide variety of questions:

(i) One can study how the geometrical properties of a single chain (its mean-square end-to-end distance, gyration radius, etc.) change as the system gets more and more dense. Scaling ideas [3] predict an interesting crossover behavior when one moves from the dilute regime (where the chains are practically still isolated from each other and hence non-interacting) to the "semidilute" regime, where the coils already interpenetrate each other but still the fraction ϕ of lattice sites occupied by the effective units of the polymer chains is rather small (e.g. $\phi \leqslant 0.1$). Sometimes one wishes to follow this behavior even further into the concentrated regime, until one ultimately reaches the case $\phi = 1$, which one feels to be most representative of a dense polymer melt or amorphous material. There is considerable interest in the properties of such dense polymer systems from the practical point of view. Clearly simulation techniques which work in the limit $\phi = 1$ are of different character (e.g. the "chain-breaking" method {fig. 2.4b, d} or the "defect-exchange"-method {fig. 2.4c}, see subsection 3.3) than methods that one can apply when the system is still rather dilute.

(ii) There is also interest in thermodynamic properties characterizing the polymer solution, such as its osmotic pressure, or the excess free energy of mixing. Such quantities are not readily obtainable from "dynamic" Monte Carlo algorithms, as described in subsections 3.1 and 3.3. Methods suitable to deal with such questions will be described in subsection 3.2: the "test chain insertion" method, as well as a method based on variation of a repulsive wall potential.

(iii) A simple variant of a grand canonical method can be applied for symmetric polymer mixtures: here the chemical potential difference between A-chains and B-chains is held fixed as an independent thermodynamical variable. So the algorithm contains "moves" by which an A-chain is transformed into a B-chain (or vice versa), while in that move the chain configuration is held fixed. This technique allows the study of phase diagrams and critical phenomena of such systems.

(iv) Other static phase transition problems that are of interest for multichain systems is the transition from disordered to ordered states of bulk polymer as a function of chain flexibility. Again the simulation may provide a stringent test of the corresponding approximate theories.

(v) Last but not least we mention questions relating to the dynamics of multichain systems. Such studies have addressed both the question of small-scale local motions, as well as trying to give a more microscopic foundation to the "reptation" concept of the tube model for polymer melts. Other work studies the freezing-in of diffusion near the glass transition, dynamics of phase separation in quenched binary polymer blends, etc.

Again we do not give a full discussion of these physical problems and the impact that simulation work has had on these questions, but refer to other reviews [10,103].

3.1. Methods with "Rouse Dynamics" vs. "Reptation Dynamics"

In principle, the extension of both the "kink-jump" method and its variants (subsection 2.2.1) and of the "slithering snake"-algorithm (subsection 2.2.2) to dense polymer lattice systems are fairly straightforward. Of course, both methods work only if the lattice does contain a sufficiently large concentration of empty sites (which we shall call "vacancies" in the following). For the "slithering snake"-algorithm, it is necessary for a vacancy to occur adjacent to the end unit of a chain at which we like to add a bond (fig. 1.4b). Thus we expect that the acceptance rate of the moves simply is proportional to ϕ_v, the volume fraction of the vacancies. Thus when ϕ_v decreases one expects that the convergence of the algorithm slows down with $\phi_v \to 0$ with relaxation times increasing at least proportional to $1/\phi_v$, since due to collective effects the possibility arises that at some ϕ_v one encounters a glass transition, where the chains get basically "locked-in", so that their self-diffusion constant vanishes (or at least becomes too small to still be "measured" in the "computer experiment"). So far, however, there does not seem much evidence for the occurrence of a glass transition when one applies the slithering snake-algorithm. Yoon and Baumgärtner [180] use simple cubic lattices of size 21^3 in their study of the order–disorder transition of chains as a function of chain flexibility and have 441 chains with $N = 20$ segments each, which implies $\phi_v = 4.8\%$. Equilibration turns out to be no problem yet. Similarly, in the study of spinodal decomposition of two-dimensional films [126] a square lattice of size 123×123 with 738 A-chains of length $N_A = 10$ and 738 B-chains of length $N_B = 10$ were used, i.e. ϕ_v as small as $\phi_v = 0.024$. In all these studies, periodic boundary conditions were used throughout. Using the bond fluctuation method a recent study obtained information on the dynamics of 2-d melts for up to $\phi_v = 0.2$ [181].

A nontrivial point is the generation of an initial configuration: It is not possible to fill the lattice so densely with chains, applying any of the "simple sampling" or "biased sampling" methods of subsection 2.1. So what usually is done is to fill the lattice with chains which are completely stretched out linearly, allowing for the suitable volume fraction of vacancies. One then has to relax this configuration carefully until the chain configurations are well equilibrated, before one starts calculating any of the desired average. In fact, this method of equilibrating chain configurations by the "slithering snake" algorithm to get a suitable initial configuration is useful and efficient also when one wants to study the dynamics of a chain with another algorithm, e.g. of the "kink-jump"-type [185]. A different approach for $d = 3$ is to implement NRRW's on the lattice and then avoid any new double occupancy of sites [116].

For a dense system of polymers moving around on the lattice by the "slithering snake" algorithm, it is interesting to analyze the dynamical properties of the chains and in particular clarify their chain length dependence. Such a study was recently attempted by Deutch [182], who studied simple cubic lattices of size 15^3 for $N = 10$, 25, 50 and 150 as well as of size 30^3 for $N = 600$. $\phi_v = 37.78\%$ was used throughout, and quantities such as the monomer-monomer displacement $\langle r^2(t) \rangle$, center of gravity displacement $\langle R_{cg}^2(t) \rangle$ and the mean square displacement $\langle s^2(t) \rangle$ of the polymer along its one arm length were estimated. If $n_f(t)$ is the number of moves accepted in the "forward" direction and $n_b(t)$ the number of moves accepted in the "backward" direction (the convention what is forward and what is backward is of course arbitrary), one defines $\langle s^2(t) \rangle$ as

$$\langle s^2(t) \rangle = \left[\left\langle (n_f(t) - n_b(t))^2 \right\rangle \right]_{av}, \tag{3.1}$$

where $[\ ]_{av}$ denotes an average over all chains in the system and many independent runs (between 6 and 100 runs [182]). It is found that $\langle r^2(t)\rangle$ for large N develops a regime where $\langle r^2(t)\rangle \propto t^a$ with a less than 1/2, while $\langle r^2(t)\rangle \propto t^1$ both at short and at long times. Similarly, both $\langle R_{cg}^2(t)\rangle$ and $\langle S^2(t)\rangle$ have in the same intermediate regime of times a behavior $\langle R_{cg}^2(t)\rangle \propto t^b$ with b less than unity, and the same holds for $\langle s^2(t)\rangle$, while a behavior proportional to the time is recovered at late times. It was suggested that this anomalous diffusion is due to a dramatic increase of the relaxation time of the chains with chain length, namely [182]

$$\tau_N \propto N^2 \exp[\text{const } N^{2/3}]. \tag{3.2}$$

If this conclusion is true it would imply that very long chains relax very slowly in dense polymer systems simulated with the "slithering snake" algorithm.

Understanding the dynamics of dense polymer systems simulated with various forms of the "kink-jump"-algorithm also turns out to be rather subtle. Again we emphasize that vacancies are needed: Both for the end-bond motion and the single-bead kink-jump a single vacancy suffices, and hence the rate of these processes goes down proportional to ϕ_v as $\phi_v \to 0$. On the other hand, we have seen in subsection 2.2.1 that these motions are not sufficient to yield a Rouse-like relaxation for single chains: The single-bead motion does not create any new bond vectors, apart from the chain ends, and hence an inclusion of the 90° crankshaft motion turns out to be crucial. At the simple cubic lattice these crankshaft motions need two adjacent empty sites: Hence we expect that for $\phi_v \to 0$ the acceptance rate of crankshaft motion trials vanishes proportional to ϕ_v^2. As a consequence of this fact, one cannot simulate as dense systems as with the slithering snake algorithm: Sariban and Binder [183,184] have studied simple cubic $L \times L \times L$ lattice with $L \leqslant 30$ and chain lengths $N \leqslant 64$ for $\phi_v \geqslant 0.4$ and $N \leqslant 32$ for $\phi_v = 0.2$; Kolinski et al. [185b] use $\phi_v = 0.5$ and very large N (up to $N = 800$), while in related very extensive work they [185a] work with somewhat smaller N ($N \leqslant 240$) but vary ϕ_v over a wide range ($\phi_v \geqslant 0.18$). For large ϕ_v ($\phi_v \geqslant 0.75$) their results still imply that the chains have a Rouse-like relaxation, $\tau_N \propto N^2$ (note that excluded volume interactions are screened out at long distances in dense polymer systems [1,3] and hence the exponent ν describing the chain linear dimensions takes again its value for ideal Gaussian chains $\nu = \frac{1}{2}$: Thus it is eq. (2.26) that must be used here and not eq. (2.29). It appears that there exists a critical vacancy concentration $\phi_v^c \approx 0.08$ where a glass transition occurs: For $\phi_v < \phi_v^c$ the chains can at best perform local motions, their center of gravity motion, however, is frozen in. For $\phi_v > \phi_v^c$ there exists a broad regime of concentrations ϕ_v, where the relaxation time seems to vary with chain length according to a power law

$$\tau_N \propto N^{a(\phi_v)}, \tag{3.3}$$

with an "effective" exponent $a(\phi_v)$ which steadily increases from its Rouse values ($a_{\text{Rouse}} = 2$) for small ϕ_v and presumably diverges as $\phi_v \to \phi_v^c$. Similar statements apply to the self-diffusion constant,

$$D_N \propto N^{-b(\phi_v)}, \tag{3.4}$$

with $b(\phi_v) = 1$ (the Rouse value) for large ϕ_v while then $b(\phi_v)$ increases as ϕ_v decreases and

presumably also $b(\phi_v \to \phi_v^c) \to \infty$. We emphasize, however, that it is not so clear that the behavior described by eqs. (3.3), (3.4) is the true asymptotic behavior valid for $N \to \infty$: It may well be that these concentration-dependent effective exponents $a(\phi_v)$, $b(\phi_v)$ are artefacts reflecting the problem that one moves through a crossover region, where the $N-$ range over which the true asymptotic behavior can be observed shrinks to zero as $\phi_v \to \phi_v^c$. In view of this uncertainty, it is also of little significance that one finds a concentration ϕ_v for which the exponents $a(\phi_v)$, $b(\phi_v)$ have values close to the experimental result in entangled melts ($a_{exp} \approx 3.4$), $b_{exp} \approx 2$ [186,187] or the prediction of the Gennes– [188] Doi–Edwards [189] tube model ($a = 3$, $b = 2$), respectively: Moreover, it is not clear why this particular concentration ϕ_v should have a particular significance. In fact, Kolinski et al. [185a,b] suggest that even when they observe $b(\phi_v) \approx 2$, the microscopic mechanism of chain motion differs significantly from the reptation-like motion in "tubes" formed by entanglement constraints in the environment: but also this conclusion is not very strong, since the data may still fall within the crossover region from Rouse to reptation behavior.

Results for the tetrahedral lattice [116,190] yield a similar picture: Since here the geometry of the lattice leads to a three-bond motion which only exchanges bond vectors as the most simple elementary move of inner segments of a chain, four-bond motions need to be added to create new bond vectors [115,116]. Since the acceptance rate of these motions vanishes as ϕ_v^2 or ϕ_v^3 as $\phi_v \to 0$, respectively, one is restricted to the use of even larger values of ϕ_v than for the sc-lattice. For $N = 200$ and $\phi_v = 66\%$ Kremer [116] still finds simple Rouse-like motion. For ϕ_v approaching ϕ_v^c one again seems to find a glass transition [190] where chains and monomers are mixed. An extensive analysis of the relaxation time for various ϕ_v and N as done by Kolinsky et al. [185] has not yet been done for the diamond lattice, however.

While neither of the studies with the kink-jump algorithms described so far has given any clear evidence for the reptation theory predictions [188,189,191], the latter have been nicely verified [116] in simulations of the motion of a chain where all surrounding chains are frozen in: Then an intermediate regime where relations $\langle r^2(t) \rangle \propto t^{1/4}$ and $\langle R_{cg}^2(t) \rangle \propto t^{1/2}$ hold is clearly identified. In this context, we also draw attention to a simulation of the motion of the "primitive path" [192] postulated in ref. [189].

Also some variants of the kink-jump method have been used: in ref. [193] the chains were allowed to backfold on themselves (for each such violation of the SAW constraint a repulsive energy u_0/k_BT was introduced, typically choosing $u_0/k_BT = 1.2$), while with respect to other chains they were strictly mutually avoiding. As pointed out later [194] this method artificially enhances the mobility for each chain to move along its own contour, and hence it is no surprise at all that this method yields a reptation-like dynamics. It is also not clear whether the static chain properties are reasonably generated by this choice of potential (where interchain and intrachain interactions differ significantly).

Meirovitch [195] has modified the kink-jump algorithm by selecting in each step randomly a group of three neighbor beads of a chain, and calculates for them the entire group of "allowed" local conformations (i.e. those that do not violate the excluded volume condition). One of these allowed local conformations is chosen randomly (if there is more than one). While it is not clear that this algorithm yields a reasonable dynamics on local scales (in contrast to the usual kink-jumps which are tried "blindly" rather than first looking which are possible), it yields a quicker equilibration of the chain configurations and is therefore probably more efficient when

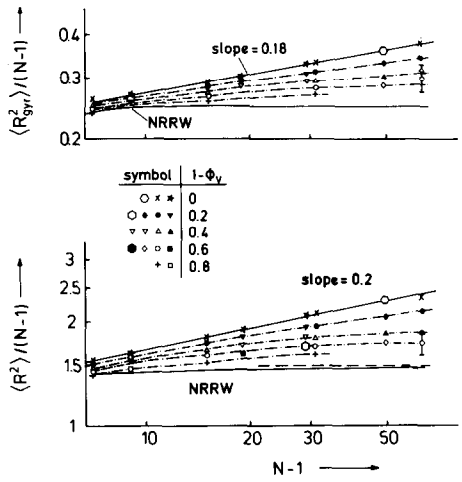

Fig. 3.1. log–log plot of the normalized gyration radius square $\langle R^2_{gyr}\rangle/(N-1)$, upper part, and the normalized squared end-to-end distance $\langle R^2\rangle/(N-1)$, lower part, versus the number of bonds $N-1$ per chain, for various concentrations of vacancies ϕ_v as indicated in the figure. Data for $N=10$, 20, 30 are due to De Vos and Bellemans [197,198] and Okamoto [199], while data for $N=50$ ar due to Olaj and Lantschbauer [200] (at $1-\phi_v=0$, 0.4, 0.6) and Okamoto [199]. All other data points are obtained by Sariban and Binder [184]. Dash-dotted curves are guides to the eye only. Full curves represent the simple power law $\langle R^2\rangle/(N-1) \propto (N-1)^{2\nu-1}$ (for $1-\phi_v=0$, the choices of the exponent $2\nu-1$ are indicated in the figure) and the exact result for the NRRW (non-reversal-random walk), respectively. Statistical errors are always smaller than the size of the symbols, except for the point $N=64$, $1-\phi_v=0.6$, where the error bar is given. From ref. [184].

one is interested in static chain properties only. An alternative technique [196] combines "slithering snake" motions with "chain-breaking" moves, see subsection 3.3.

Of course, since neither the "slithering-snake" algorithm nor the kink-jump algorithm are ergodic already for single chains (see subsection 2.2), they are not ergodic either for multichain systems. For any of the chains, certain "forbidden" configurations are never reached. Again the general belief is that the statistical weight of these inaccessible states is negligibly small, and hence this problem does not matter in practice. Fig. 3.1 presents some evidence in favour of this belief: Results due to a variety of authors [106,184,185,197–199], which apply different techniques, are combined there, and it is seen that the results always agree within the statistical errors. Ref. [199] applied the slithering snake technique, the other papers apply all kink-jump type techniques but differ in their details: E.g., ref. [184] includes less types of motions than [185], but generates initial configurations by "biased sampling" techniques, and takes an average over runs starting from several initial configurations. Thus for the chain lengths considered in fig. 3.1 and within the restricted accuracy of these data (very roughly, the relative error is 1%) any reservations about the nonergodicity of the algorithms are not relevant. Also for multichain systems the use of bond fluctuation methods may be attractive. There one can go to very high densities. There blocked configurations only can exist as a finite size effect of the box, which are then in the course of a simulation trivially to identify.

3.2. "Grand canonical" simulation of many-chain systems

In subsection 2.2, we have encountered the simulation of single chains in the grand canonical ensemble, where the chain length N was fluctuating and rather *the chemical potential of the effective units* was the independently given thermodynamic variable. In principle, this technique could be applied to a system containing many chains, too. In practice, we are not aware of any applications of this technique: Presumably, the resulting "polydispersity" (chain length distribution) of the resulting system is considered a serious disadvantage.

However, in a multichain system where all chains have precisely the same chain length N we can introduce a *chemical potential μ which is the thermodynamic variable conjugated to the number of chains n in our system*. If we fix μ rather than n, the latter variable would be statistically fluctuating: The Monte Carlo algorithm then contains moves, where chains are randomly removed from the system or added to the system, in accord with the prescribed transition probability.

Since any chain that is inserted into the system as a whole must obey the excluded volume constraint with all the other chains present in the system, this method can work only if the polymer concentration is still very small. Otherwise all chain insertion trials are never successful – but $\langle n \rangle$ as well as $\langle n^2 \rangle - \langle n \rangle^2$ can be sampled reasonably well only if a large number of chain insertions has been successfully performed.

A variant of this method which in principle suffers from the same problem but in practice seems to work slightly better is Okamoto's [199–205] test chain insertion method, which is essentially based on the same idea as Widom's [206] particle insertion method for ordinary fluids. This method tries to obtain the chemical potential from a calculation in the canonical ensemble (n fixed) by sampling the expectation value of the acceptance rate of a move where a test chain would be inserted into the system somewhere (in contrast to the really grand-canoncial simulation the chain insertion is not carried out even if the move is "accepted"). The chemical potential μ then is obtained from the relation

$$\mu = -k_B T \ln\langle \exp(-U_t/k_B T)\rangle_n$$

where U_t is the energy of the inserted particle and $\langle\ \rangle_n$ means the ensemble average over the n particle system.

An interesting alternative method was recently proposed by Dickman [207], relating the pressure of the system to the segment density at a repulsive wall. One considers a d-dimensional cubic lattice, of length L in $d-1$ dimensions and of length H in the remaining direction, with which one associates the coordinate x. There is an infinite repulsive potential at $x = 0$ and $x = H + 1$, in the other directions periodic boundary conditions apply. The partition function of n N-mers on the lattice then is $Z(N, n, L, H) = (n!)^{-1} \Sigma \exp(-u/k_B T)$, where the sum runs over all chain configurations on the lattice, and the potential U incorporates restrictions which define the chain structure, prohibit overlaps, etc. While in a continuous-space model the pressure is $\pi^* = \partial[\ln Z(N, n, L, H)]/\partial V = L^{-(d-1)}\, \partial[\ln Z(N, n, L, H)]/\partial H$, the analogous expression for the lattice model is

$$\pi^* = L^{-(d-1)}[\ln Z(N, n, L, H) - \ln Z(N, n, L, H-1)]. \tag{3.5}$$

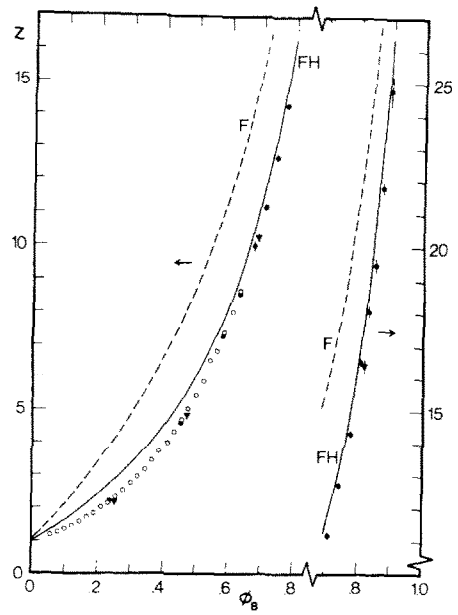

Fig. 3.2. The compressibility factor z of athermal 20-mers on the square lattice plotted vs the bulk density ϕ_B. Open circles: test chain insertion method [206]; filled circles: wall density method [208], using a cell with linear dimensions $L = 30$, $H = 60$. Triangles: same as filled circles except that $H = 30$. From ref. [208].

The difference of free energies required in this equation now is evaluated by associating with each occupied site in the plane $x = H$ a factor λ, $0 < \lambda < 1$; it may be viewed as being due to an additional finite repulsive potential next to the wall. Denoting the number of occupied sites in the plane $x = H$ as $N(H)$ we obtain the partition function as

$$Z(N, n.L, H, \lambda) = (n!)^{-1} \sum \exp(-U/k_B T) \lambda^{N(H)}. \tag{3.6}$$

Since $Z(N, n, L, H, 1) = Z(N, n, L, H)$ and $Z(N, n, L, H, 0) = Z(N, n, L, H-1)$, we get

$$\pi^* = L^{-(d-1)} \int_0^1 \left(\frac{\partial \ln Z}{\partial \lambda} \right) \mathrm{d}\ell = \int_0^1 \frac{\mathrm{d}\lambda}{\lambda} \varphi_H(\lambda), \quad \varphi_H(\lambda) \equiv N(H) L^{d-1}. \tag{3.7}$$

Thus one carries out simulations for several values of λ, samples $\varphi_H(\lambda)$, the fraction of occupied sites in the plane $x = H$, and performs the integral in eq. (3.7) numerically. Fig. 3.2 shows as an example of the usefulness of both this method and the test chain insertion method [205] a calculation of the "compressibility factor" $z = N\pi^*/\phi_B$, ϕ_B being the density in the bulk, for $N = 20$. The data are compared to the mean-field results of Flory [1,208] and Huggins [209],

$$z_F = 1 - \frac{N}{\phi_B} \left[\ln(1 - \phi_B) + \phi_B \right], \tag{3.8}$$

$$z_{FH} = z_F + \frac{2N}{\phi_B} \left\{ \ln\left[1 - \tfrac{1}{2}\phi_B (1 - 1/N) \right] + \tfrac{1}{2}\phi_B (1 - 1/N) \right\}. \tag{3.9}$$

It is seen that z_F is rather unsatisfactory, while the Huggins result z_{FH} is in rather close agreement with the data at high densities.

Both in the "test chain insertion method" and in the "wall density method" the chain configurations were sampled with the "slithering snake" technique. A different approach has been taken by the Russian group [210] who generate multi-chain ensembles by biased sampling (the Rosenbluth–Rosenbluth [30,31] technique), and by Öttinger [52,211] who employed the Meirovitch technique [49–51] of "scanning future steps". While the latter method seems to yield useful results particularly for not too concentrated systems ("semi-dilute solutions" [3]), we view the reliability of the former as being somewhat uncertain (compare the evaluation of errors which occur in this method already for single chains, see subsection 2.1.2).

A truly grand canonical simulation can be performed for symmetrical binary polymer mixtures (in the presence of vacancies) [183,184]. There the quantity of interest is the difference in number between A-chains and B-chains, $\Delta n = n_A - n_B$, or the relative volume fraction $\phi = n_A/(n_A + n_B)$ of one component. The conjugate thermodynamical variable is then a chemical potential difference $\Delta\mu$ between the two species. Holding $\Delta\mu$ fixed the total number of chains $n = n_A + n_B$ does not change but one must allow for moves where an A-chain transforms into a B-chain and vice versa. If the mixture is symmetric ($N_A = N_B$), the excluded volume interaction is not affected by these moves at all, and only the finite energies between neighboring AA, AB, BB pairs of monomers (ϵ_{AA}, ϵ_{AB}, ϵ_{BB}) have to be considered in the transition probability, together with $\Delta\mu$. To equilibrate the single-chain configuration themselves, in between these moves just described the chains relax by the "kink-jump" method [183,184] (the slithering snake algorithm could be used as well). By this technique it has been possible to study critical phenomena associated with the unmixing of polymer mixtures. Fig. 3.3 presents as an example the order parameter $m = \langle |\Delta n| \rangle/n$ and the specific heat C as a function of temperature $k_B T/\epsilon$ [where $\epsilon = -\epsilon_{AA} = -\epsilon_{BB}$ in this case and $\epsilon_{AB} = 0$], for $\phi_v = 0.2$ and $N = 16$ and simple cubic $L \times L \times L$ lattices, with box-sizes varying from $L = 10$ to $L = 20$. As is well-known in the study of phase transitions with Monte Carlo methods [212–215], pronounced finite-size effects are inevitably present, as is also evident from fig. 3.3, and must be taken into account in a finite-size-scaling analysis [214,216] in order to extrapolate reliably to the thermodynamic limit. These techniques are well established and have been reviewed recently elsewhere [215,216] and hence will not be discussed further here. Again such results are very useful to check the accuracy of approximate theories: Fig. 3.4 shows that the approximation of Flory [1,208] overestimates the critical temperature at all chain lengths and vacancy concentrations by at least a factor of two, while the approximation due to Guggenheim [209] (available only for $\phi_v = 0$) is somewhat better. The dramatic breakdown of the Flory theory for small $1 - \phi_v$ and the purely repulsive interactions ($\epsilon_{AA} = \epsilon_{BB} = 0$, $\epsilon_{AB} \neq 0$) presents evidence for the prediction due to Joanny et al. [218] that in the limit $1 - \phi_v \to 0$, $N \to \infty$ the two polymer species become effectively compatible at all temperatures.

3.3. "Chain-breaking" methods

In this subsection we are describing methods that have been proposed to handle very dense lattice systems [196,106,107,105] including the limit where no vacancies are present. While Refs. [106,107] accept a very high degree of "polydispersity" (rather than having a "monodisperse"

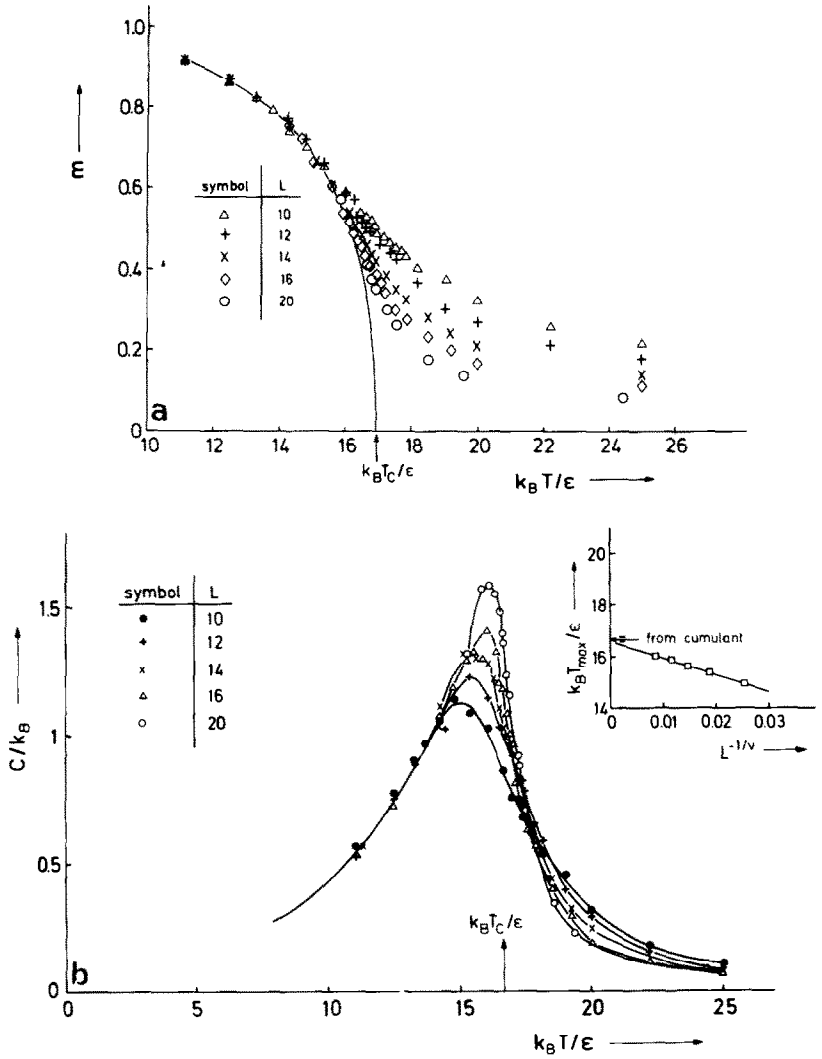

Fig. 3.3. Order parameter (a) and specific heat (b) of a symmetrical polymer mixture with $N_A = N_B = N = 16$ and $\phi_V = 0.2$ plotted vs. temperature k_BT/ϵ, for various sizes L of the simple cubic lattice as indicated in the figure. The critical temperature is estimated either from an extrapolation of the peak position of the specific heat versus $L^{-1/\nu}$ ($\nu \approx 0.63$ being the correlation length exponent [215,216]) or from locating the common intersection temperature of the "cumulants" $U_L(T) \equiv 1 - \langle(\Delta n)^4\rangle/[3\langle(\Delta n)^2\rangle^2]$ for the various L. From ref. [183].

system with chains of uniform chainlength N, a distribution of chainlengths is created by the algorithm), the degree of polydispersity is a controllable parameter in refs. [196,106], and ref. [196,106], and ref. [105] (the so-called COMO ("collective motion") algorithm) allows to simulate strictly monodisperse multichain systems.

Both refs. [106,107] include motions of the "bond flip"-type (fig. 2.4B), where a pair of parallel bonds is rotated if the bonds belong to neighboring chains. If the two bonds belong to the same chain, this move is forbidden since it would lead to "cyclization" (i.e., ring formation).

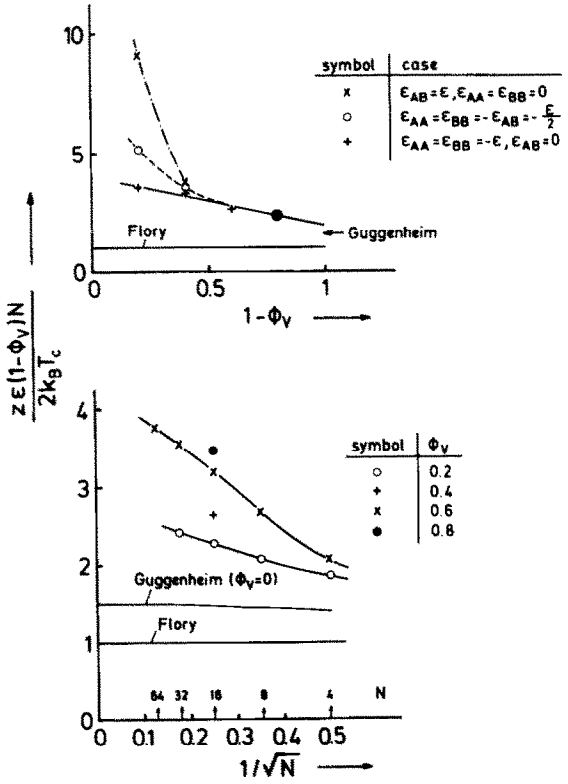

Fig. 3.4. Normalized inverse critical temperature plotted versus the polymer concentration $1-\phi_v$ (upper part) and versus the inverse of the square root of the chain length (lower part), for the model of a symmetrical polymer mixture on the simple cubic lattice (cf. fig. 3.3). The normalization of T_c is chosen such that the Flory prediction of the critical temperature is divided by the actual T_c. Upper part refers to $N=16$ (note that for $1-\phi_v=0.8$ all three cases yield the same T_c (full dot)). Curves are only drawn to guide the eye. From ref. [184].

This motion does not involve the chain ends of either chain. The second move common to both refs. [106,107] is the so-called "end attack" (fig. 2.4D): From a site of a chain that is nearest neighbor to a chain end of another chain a bond is rotated so that the previous chain end is now an inner bead of one of the chains, and the site from which the bond moved away becomes a chain end. Ref. [107] considers also intramolecular end attacks (the so-called "backbite move"), if it does not lead to cyclization. On the other hand, ref. [106] includes another reaction between two adjacent chain ends: The chains may "dimerize" at this bond and subsequently are subject to a chain scission at a statistically chosen bond. This reaction ensures a rapid migration of end segments.

Obviously, these reactions by which chains are "broken" and reconnected again in a different fashion do not conserve chain lengths. If no further restriction is introduced, the resulting distribution of chain lengths turns out to be extremely broad. Mansfield [107] therefore forbids any reactions, by which chains shorter than some given length N_{min} would be created. Typically he was choosing $N_{min} \approx \frac{1}{2}\overline{N}_n$, $\overline{N}_n$ being the number-average of the chain length distribution. Madden [196] works at densities $\phi \approx 0.8$ to 0.9 in the "bulk" of his systems (he was studying

interfacial properties also, and the density in the interfacial region is much smaller, of course), and thus also "slithering snake" motions could be included; in addition, he introduces both an upper and a lower cutoff, so that the chain lengths lie in an interval $N_{\min} \leqslant N \leqslant N_{\max}$. It turns out that the distribution of chain lengths generated by this method is rather close to a rectangular distribution, which is rather different from the experimentally relevant distributions (which are often well approximated by a log–normal distribution [219].)

Still a different idea to control the degree of polydispersity was applied by Olaj and Lantschbauer [106]. If ΔN_{old} is the absolute value of the difference of chain lengths in the chain pair before the reaction and ΔN_{new} after the (trial reaction, the new configuration will be accepted always if $\Delta N_{\text{new}} \leqslant \Delta N_{\text{old}}$. On the other hand, if $\Delta N_{\text{new}} > \Delta N_{\text{old}}$, the new configuration is accepted with probability of $\exp[-f(\Delta N_{\text{new}} - \Delta N_{\text{old}})]$ only, otherwise the old configuration is retained. The parameter f controls the width of the distribution of chain lengths. Choosing $f = 10/N$ yields a chain length distribution of a shape qualitatively similar to experiment and a "polydispersity index" $\overline{N}_{\text{w}}/\overline{N}_{\text{n}}$ ("weight average"/"number average") of about 1.02, i.e. monodisperse for practical purposes. Although most of the calculations of ref. [106] were done for $f = 0$, i.e., an extremely polydisperse distribution of chain lengths, a comparison performed for $\overline{N}_{\text{n}} = 50$ shows that both $\langle R^2 \rangle$ and $\langle R^2_{\text{gyr}} \rangle$ vary by far less than 1% when $\overline{N}_{\text{w}}/\overline{N}_{\text{n}}$ varies from 1.686 to 1.015. Furthermore, the results of ref. [106] are nicely consistent with a smooth monotonous extrapolation of radii obtained at $\phi_{\text{v}} < 1$ by the kink-jump technique for the strictly monodisperse case [106,184]. In contrast, the COMO algorithm which is based on exchanging crankshafts between pairs of chains (fig. 2.4C) or generalizations of such exchanges involving loops containing three or more chains [105], yields less satisfactory results for the chain radii, although a monodisperse chainlength distribution is strictly conserved by this algorithm: e.g. for $N = 16$ and $\phi = 1$ the radii are distinctly larger than those obtained by the kink-jump method for $\phi = 0.6$ and $\phi = 0.8$ [184]. This result does not make sense, since with increasing ϕ the radii should decrease monotonically, but must not increase. Presumably this failure of the method of ref. [105] is due to the very slow relaxation noted [105] for this algorithm. However, it is also possible that this algorithm (as well as the other algorithms of this section) suffer from more basic problems, such as lack of ergodicity: As noted in ref. [107] ergodicity is neither easily proved nor disproved for these algorithms in dense multichain systems.

In conclusion, we feel that these chain-breaking methods of Olaj, Mansfield and co-workers [106,107] yield reliable results for the chain linear dimensions in very dense configurations, and that polydispersity is not really a problem in practice. The available data are roughly consistent with the expected variation $\langle R^2 \rangle \propto N$ for large N [1,3], and agree quantitatively with chain configurations under θ-conditions [107].

4. Conclusions

The previous chapters gave a short introduction into the lattice Monte Carlo techniques for polymers. On purpose we confine ourselves to lattice models. Of course, besides the examples already mentioned, there exist several approaches using other methods than Monte Carlo. E.g., Ceperly et al. [220] use a Brownian Dynamics method to study the properties of dense polymer systems, as well as chains in solution. More recently even molecular dynamis was used to study

single chains and melts [221,222] as well as stars [176]. We again want to emphasize that our main purpose was to discuss the technical aspects of polymer simulations. For single chains the techniques are rather well developed and a variety of approaches exist. For more complicated systems, e.g. branched structures or many chain systems, we are still in the early stage of large scale applications. We think that a careful use of lattice Monte Carlo together with other numerical approaches (continuum MC, molecular dynamics, Brownian dynamics) for the future will become increasingly important. Especially the more scientists are becoming interested in more complex systems, such computer simulations will be one of the very powerful tools applied.

Acknowledgements

This research is supported in part by the Deutsche Forschungsgemeinschaft (Sonderforschungsbereiche 41/S38, 262/D1). It is a pleasure to thank I. Batoulis. A. Baumgärtner, I. Carmesin, F. van Dieren, J.W. Lyklema and A. Sariban for their fruitful collaboration on parts of the research described here. We are grateful to a large number of colleagues supplying us steadily with preprints of their work, which helped to keep this review reasonably up-to-date.

References

[1] P.J. Flory, Principles of Polymer Chemistry (Cornell University Press, Ithaca, New York, 1953).
[2] P.J. Flory, Statistical Mechanics of Chain Molecules (Interscience, New York, 1969).
[3] P.G. de Gennes, Scaling Concepts in Polymer Physics (Cornell University Press, Ithaca, New York, 1979).
[4] H. Yamakawa, Modern Theory of Polymer Solutions (Harper and Row, New York, 1971).
[5] E.W. Montroll, J. Chem. Phys. 18 (1950) 734.
[6] G.W. King, Nat. Bur. Stand. Appl. Math. Ser. 12 (1951).
[7] F.T. Wall and F.T. Hioe, J. Chem. Phys. 74 (1970) 4410, 4416.
[8] P. Grassberger, Z. Phys. B 48 (1982) 255 (SAW-polygons meanwhile are enumerated up to $N = 48$ steps: J.G. Enting and A.J. Guttmann, J. Phys. A 18 (1985) 1007).
[9] C. Domb and F.T. Hioe, J. Chem. Phys. 51 (1969) 1915.
[10] For a recent review on applications, see A. Baumgärtner, in: Applications of the Monte Carlo Method in Statistical Physics ed. K. Binder, (Springer, Berlin, Heidelberg, New York, 1984) chap. 5.
[11] Early work is reviewed by F.T. Wall, S. Windwer and P.J. Gans, in: Methods in Computational Physics, vol. 1, eds. B. Alder, S. Fernbach and M. Rotenberg (Academic Press, New York, 1983).
C. Domb, Advan. Chem. Phys. 15 (1969) 229.
See also J.M. Hammerlsey and D.C. Handscomb: Monte Carlo Methods (Chapman and Hall, London, third print 1983).
D.S. McKenzie Phys. Rep. 27 (1976) 1.
[12] M. Doi and S.F. Edwards, Theory of Polymer Dynamics (Clarendon Press, Oxford, 1986).
[13] P.G. de Gennes, Phys. Lett. A 38 (1972) 339.
[14] B. Nienhuis, Phys. Rev. Lett. 49 (1982) 1062.
[15] Le Guillou and Zinn-Justin, Phys. Rev. Lett. 39 (1977) 95; Phys. Rev. B 21 (1980) 3976.
[16] For the ϕ^4 model see A. Milchev, K. Binder and D.W. Heermann, Z. Phys. B 63 (1986) 521.
For percolation see e.g. D. Stauffer. Introduction to Theory (Taylor and Francis, London, 1985) for walks see ref. [33].
[17] Since these are ratios of critical amplitudes, they are independent of the lattice but not of the dimensions. The actual data are taken from ref. [27] for the fcc lattice.

[18] M.J. Stephen, Phys. Lett. A 53 (1975) 363.
[19] P.G. de Gennes, J. de Phys. Lett. 36 (1979) 55.
[20] M. Janssens and A. Bellemans, J. Phys. A 8 (1975) L 106.
[21] K. Kremer, A. Baumgärtner and K. Binder, J. Phys. A 15 (1982) 2879.
[22] B.J. Cherayill, J.F. Douglas and K.F. Freed, J. Chem. Phys. 87 (1987) 3089. This contains a discussion of the discrepancies between the binary cluster integral and the osmotic second virial coefficient between chains.
[23] F.T. Wall, L.A. Hiller and W.F. Atchison, J. Chem. Phys. 23 (1955) 913, 23 (1955) 2314, 26 (1957) 1742.
[24] S. Windwer, in: Marcov Chains and Monte Carlo Calculations in Polymer Science, ed. G.G. Cowry (Dekker, New York, 1970).
[25] M.G. Watt, J. Phys. A 8 (1975) 61.
[26] G.F. Lawler, Duke, Math. J. 47 (1980) 655, 53 (1986) 249.
[27] J. Batoulis and K. Kremer, J. Phys. A 21 (1988) 127.
[28] J.W. Lyklema and K. Kremer, Phys. Rev. B 31 (1985) 3182.
[29] J. Mazur, J. Chem. Phys. 40 (1964) 1001.
J. Mazur and P. Joseph, J. Chem. Phys. 38 (1963) 1292.
[30] M.N. Rosenbluth and A.W. Rosenbluth, J. Chem. Phys. 23 (1955) 356.
[31] J.M. Hammersley and K.W. Morton, J. Roy. Stat. Soc. (B) 16 (1954) 23.
[32] N.C. Smith and R.J. Fleming, J. Phys. A 8 (1975) 929.
[33] J.W. Lyklema and K. Kremer, J. Phys. A 19 (1985) 279 and references therein.
[34] I. Majid, N. Jan, A. Coniglio and H.E. Stanley, Phys. Rev. Lett. 52 (1984) 1257.
[35] F.L. Mc Crackin, J. Res. Nat. Bur. Stand. Sect. B 76 (1972) 193.
[36] J. Mazur and F.L. Mc Crackin, J. Chem. Phys. 49 (1968) 648.
[37] F.L. Mc Crackin, J. Mazur and C.L. Guttmann, Macromolecules 6 (1973) 859.
[38] R. Finsy, M. Janssens and A. Bellemans, J. Phys. A 8, L 106 (1975).
[39] L. Pieliti, J. de Phys. Lett. 45 (1984) L 925.
L. Pietronero, Phys. Rev. Lett. 55 (1985) 2025.
C. Guttmann, Macromolecules 19 (1986) 833.
[40] B. Duplantier, Europhys. Lett. 1 (1986) 491 and references therein.
[41] J.W. Lyklema and K. Kremer, unpublished data (1986).
[42] T.M. Birshtein, S.U. Buldyrev and A.M. Elyaskevitch, 26 (1985) 1815.
[43] K. Kremer and J.W. Lyklema, Phys. Rev. Lett. 54 (1985) 267; J. Phys. A 18 (1985) 1515.
[44] T.M. Birshtein, A.M. Skvortsov and A.A. Sariban, Polymer 24 (1983) 1145.
[45] K. Kremer, PhD Thesis, unpublished (1983).
[46] E. Eisenriegler, K. Binder and K. Kremer, J. Chem. Phys. 77 (1982) 6292.
[47] K. Kremer, J. Chem. Phys. 83 (1985) 5882.
[48] F.T. Wall, R.J. Rubin and L.M. Isaacson, J. Chem. Phys. 27 (1957) 186.
[49] H. Meirovitch, J. Phys. A 15 (1982) 735.
[50] H. Meirovitch, Macromolecules 16 (1983) 249.
[51] H. Meirovitch, J. Chem. Phys. 79 (1983) 502.
[52] H.C. Öttinger, Macromolecules 18 (1985) 93.
[53] H. Meirovitch, Macromolecules 16 (1983) 249, 1628.
[54] H. Meirovitch, Macromolecules 18 (1985) 563, 569.
[55] K.E. Schmidt, Phys. Rev. Lett. 51 (1983) 2175.
[56] H. Meirovitch, Phys. Rev. A 32 (1985) 3709.
H. Meirovitch and N.A. Scheraga, J. Chem. Phys. 84 (19860 6369.
[57] Z. Alexandrovicz, J. Chem. Phys. 51 (1969) 561.
[58] K. Suzuki, Bull. Chem. Soc. Japan 41 (1968) 538.
[59] This line of arguments is based on an unpublished note of T.A. Witten, Y. Kantor and K. Kremer.
[60] N. Madras and A.D. Sokal, J. Stat. Phys. 50 (1988) 109.
[61] Z. Alexandrovicz and Y. Accad, J. Chem. Phys. 54 (1971) 5338.
[62] Z. Alexandrovicz and Y. Accad, Macromolecules 6 (1973) 251.
[63] C. Domb and G.S. Joyce, J. Phys. C 5 (1972) 956.

[64] Z. Alexandrovicz, Phys. Rev. Lett. 50 (1983) 736.
[65] J. Batoulis, in preparation (1987).
[66] J. Batoulis and K. Kremer, preprint (1988).
[67] Y. Chen, J. Chem. Phys. 74 (1981) 2034.
[68] F.T. Wall and J.J. Erpenbeck, J. Chem. Phys. 30 (1959) 634, 637.
[69] M. Lax and J. Gillis, Macromolecules 10 (1977) 334.
[70] C. Brender, D. Ben-Avraham and S. Havlin, J. Stat. Phys. 31 (1983) 661.
[71] F.T. Wall, S. Windwer and P.J. Gans, J. Chem. Phys. 37 (1962) 1461.
[72] A.J. Barrett and A. Pound, J. Phys. A 14 (1980) 1811.
[73] A.J. Barrett and D.L. Tremain, Macromolecules 20 (1987) 187.
[74] R.P. Smith, J. Chem. Phys. 38 (1963) 1463.
[75] H.L. Frisch, F.C. Collins and B. Friedman, J. Chem. Phys. 19 (1951) 1402.
[76] J.M. Hammersley and K.W. Morton, J. Roy. Stat. Soc. B 16 (1954) 23.
[77] G.F. Lawler, J. Phys. A 20 (1987) 4565.
[78] J.W. Lyklema and C. Evertsz, J. Phys. A 19 (1986) L 895.
J.W. Lyklema, C. Evertsz and C. Petronero, Europhys. Lett. 2 (1986) 77.
[79] D.C. Rapaport, J. Phys. A 18 (1985) 113.
[80] D.C. Rapaport, J. Phys. A 18 (1985) L 39; Phys. Rev. B 30 (1984) 2906.
[81] N. Metropolis, A.W. Rosenbluth, M.N. Rosenbluth, A.N. Teller and E. Teller, J. Chem. Phys. 21 (1953) 1087.
[82] H. Müller-Krumbhaar and K. Binder, J. Stat. Phys. 8 (1973) 1.
[83] P.E. Rouse, J. Chem. Phys. 21 (1953) 1272.
[84] P.H. Verdier and W.H. Stockmayer, J. Chem. Phys. 36 (1962) 227.
[85] P.H. Verdier, J. Chem. Phys. 45 (1966) 2122.
[86] P.H. Verdier, J. Chem. Phys. 52 (1970) 5512.
[87] P.H. Verdier, J. Chem. Phys. 59 (1973) 6119.
[88] H.J. Hilhorst and J.M. Deutch, J. Chem. Phys. 63 (1975) 5153.
[89] H. Boots and J.M. Deutch, J. Chem. Phys. 67 (1977) 4608.
[90] D.E. Kranbuehl and P.H. Verdier, J. Chem. Phys. 71 (1979) 2662.
[91] P.H. Verdier and D.E. Kranbuehl, Polymer Preprints (ACS) 17, No .2 (1976) 148.
[92] D.E. Kranbuehl and P.H. Verdier, Polymer Preprints (ACS) 21, No. 2 (1980) 195.
[93] K. Kremer, J. Pol. Sc. Pol. Symp. 73 (1985) 157.
[94] D.E. Kranbuehl and P.H. Verdier, preprint.
[95] S. Caracciolo and D.A. Sokal, J. Phys. A 19 (1986) L 797.
[96] R. Zwanzig and N.K. Ailawadi, Phys. Rev. 182 (1969) 280.
[97] H. Müller-Krumbhaar and D.P. Landau, Phys. Rev. B 14 (1976) 2014.
[98] A. Berretti and A.D. Sokal, J. Stat. Phys. 40 (1985) 483.
[99] S. Wansleben and D.P. Landau, J. Appl. Phys. 61 (1987) 3968.
S.Y. Tang and D.P. Landau, Phys. Rev. B 36 (1987) 567.
D.P. Landau and S. Wansleben, preprint.
[100] B. Berg and D. Foerster, Phys. Lett. B 106 (1981) 323.
[101] C. Aragão de Carvalho and S. Caracciolo, J. de Phys. 44 (1983) 323.
[102] C. Aragão de Carvalho, S. Caracciolo and J. Fröhlich, Nucl. Phys. B 215 [FS7], (1983) 209.
[103] A. Baumgärter, Ann. Rev. Phys. Chem. 35 (1984) 419.
[104] P.C. Hohenberg and B.I. Halperin, Rev. Mod. Phys. 49 (1977) 435.
[105] T. Pakula and S. Geyler, preprint.
[106] O.F. Olaj and W. Lantschbauer, Makromol. Chem., Rapid Commun. 3 (1982) 847.
[107] M.L. Mansfield, J. Chem. Phys. 77 (1982) 1554.
[108] R.A. Orwoll and W.H. Stockmayer, Advan. Chem. Phys. 15 (1969) 305.
[109] K. Iwata and M. Kurata, J. Chem. Phys. 50 (1969) 4008.
K. Iwata, J. Chem. Phys. 54 (1971) 12.
[110] M. Lax and C. Brender, J. Chem. Phys. 67 (1977) 1785.
[111] A. Baumgärtner and K. Binder, J. Chem. Phys. 71 (1979) 2541.

[112] N. Madras and A.E. Sokal, J. Stat. Phys. 47 (1987) 573.
[113] P.H. Verdier, J. Comput. Phys. 4 (1969) 204.
[114] O.J. Heilmann, Mat. Fys. Medd. Dan. Vid. Selsk. 37 (1968) 2.
[115] F. Geny and L. Monnerie, J. Polym Sci. Phys. Ed. 17 (1979) 131.
[116] K. Kremer, Macromolecules 16 (1983) 1632.
[117] D.J. Heilmann and J. Rotner, J. Stat. Phys. 27 (1982) 19.
[118] A. Baumgärtner, K. Kremer and K. Binder, Faraday Discuss. Chem. Soc. 18 (1983) 37.
[119] A. Sadiq and Y. Khwaja, Z. Phys. B 42 (1981) 163.
Y. Khwaja and A. Sadiq, J. Polym. Sci. Polym. Phys. Ed. 19 (1981) 499.
[120] M.T. Gurler, C.C. Crabb, D.M. Dahlin and J. Kovac, Macromolecules 16 (1983) 398.
[121] P. Romiszowski and W.H. Stockmayer, J. Chem. Phys. 80 (1984) 485.
[122] A.K. Kron, Polymer Sci. USSR 7 (1965) 1361.
A.K. Kron and O.B. Ptitsyn, Polym. Sci. USSR 9 (1967) 847.
A.K. Kron, O.B. Ptitsyn, A.M. Skvortsov and A.K. Fedorov, Molec. Biol. 1 (1967) 487.
[123] F.T. Wall and F. Mandel, J. Chem. Phys. 63 (1975) 4592.
F. Mandel, J. Chem. Phys. 70 (1979) 3934.
[124] J.R. Banavar and M. Muthukumar, Chem. Phys. Lett. 93 (1982) 35.
M. Muthukumar, J. Stat. Phys. 30 (1983) 457.
[125] M.E. Fisher, Rev. Mod. Phys. 46 (1974) 597.
[126] A. Baumgärtner and D.W. Heermann, Polymer 27 (1986) 1777.
[127] M. Lal, Molec. Phys. 17 (1969) 57.
[128] O.F. Olaj and K.H. Pelinka, Makromol. Chem. 177 (1976) 3413.
[129] B. Mac Donald, N. Jan, D.L. Hunter and M.O. Steinitz, J. Phys. A 18 (1985) 2627.
[130] D.L. Hunter, N. Jan and B. Mac Donald, J. Phys. A 19 (1986) L 543.
[131] I. Carmesin and K. Kremer preprint, Macromolecules in press (1988).
[132] Y. Kantor, M. Kardar and D.R. Nelson, Phys. Rev. A35 (1987) 3056.
[133] K. Kremer and K. Binder, J. Chem. Phys. 81 (1984) 6381.
[134] I. Carmesin and K. Kremer, Proc. of the ILL Workshop on Polymer dynamics, Grenoble (1987), to be published in Proc. in Phys. (Springer, Heidelberg, 1988).
[135] S. Redner and P.J. Reynolds, J. Phys. A 14 (1981) 2679.
[136] D. Dhar and P.M. Lam, J. Phys. A 19 (1986) L 1057.
[137] M.E. Fisher, V. Privman and S. Redner, J. Phys. A 17 (1984) L 569.
[138] S. Redner and V. Privman, J. Phys. A 20 (1987) L 857.
[139] V. Privman and S. Redner, preprint (1988).
[140] For a general overview of gelation phenomena see e.g. M. Adam and D. Stauffer, Advan. Pol. Sc. 44 (1982) 103.
[141] The various classes of kinetic growth models which may have application to polymers are covered by the following reviews and books:
– H. Herrmann, Phys. Rep. 136 (1986) 155.
– F. Family and D.P. Landau, eds. Kinetics of aggregation and gelation (Elsevier, Amsterdam, 1984).
– N. Ostrowski and H.E. Stanley, eds. Growth and Form (Nijhoff, Boston, 1986).
[142] B.H. Zimm, Macromolecules 13 (1980) 592.
[143] For a general discussion of such questions see ref. [15] and refs therein.
[144] See e.g. A.J. Guttmann, J. Phys. A 17 (1984) 455. J. Majid, Z.V. Djordjevic and H.E. Stanley, Phys. Rev. Lett. 51 (1983) 143 and references therein.
[145] J.W. Lyklema and K. Kremer, Phys. Rev. B 31 (1985) 3182.
[146] D.C. Rapaport, Phys. Rev. B 30 (1984) 2906; J. Phys. A 18 (1985) L 39; J. Phys. A 18 (1985) 113.
[147] S. Havlin and D. Ben Avraham, Phys. Rev. A 27 (1983) 2759; J. Phys. A 15 (1982) L 317.
[148] S. Havlin and D. Ben Avraham, J. Phys. A 15 (1982) L 311, L 321, Phys. Rev. A 26 (1982) 1728.
[149] J.P. Cotton, D. Decker, B. Farnoux, G. Jannink, R. Ober and C. Picot, Phys. Rev. Lett. 32 (1974) 1179.
[150] T.W. Burkhardt and van Leeuwen, eds. Real Space Renormalization Group (Springer, Heidelberg, 1982).
[151] K. Kremer, A. Baumgärtner and K. Binder, Z. Phys. B 40 (1981) 331.
A. Baumgärtner, J. Phys. A 13 (1980) L 39.

[152] A. Baumgärtner, J. de Phys. 43 (1982) 1407.
[153] T.M. Birshtein, A.M. Skvortsov and A.A. Sariban, Macromolecules 9 (1976) 888.
[154] Y. Chen, J. Chem. Phys. 74 (1981) 2034, 75 (1981) 2447, 5160.
[155] G. Ten Brinke and G. Hadziiaonnou, Macromolecues (1987).
[156] J.P.J. Michels and F. Wiegel, Phys. Lett. A 90 (1982) 381. M. Bishop and J.P.J. Michels, J. Chem. Phys. 82 (1985) 1059.
[157] A.T. Clark and M. Lal, J. Chem. Soc. Faraday Trans. 2, 77 (1981) 981 and refs. therein.
[158] F.T. Wall, F. Mandel and J.C. Chin, J. Chem. Phys. 65 (1976) 2231.
[159] J. Webmann, J.L. Lebowitz and M.N. Kalos, J. de Phys. 41 (1980) 579.
[160] F.L. Mc Crackin, J. Chem. Phys. 47 (1967) 1980.
[161] F. van Dieren and K. Kremer, Europhys. Lett. 4 (1987) 569.
[162] T. Cosgrove, T. Heath, B. van Leut, F. Leermakers and J.M.J. Scheutjens, Macromolecules 20 (1987) 1692.
[163] S. Lione and H. Meirovitch, J. Chem. Phys. 88 (1988) 4498.
H. Meirovitch and S. Lione, J. Chem. Phys. 88 (1988) 4507.
[164] K. Kremer, Z. Phys. B 45 (1981) 149.
[165] A. Baumgärtner and M. Muthukumar, J. Chem. Phys. 87 (1987) 3082.
[166] B.H. Zimm and W.H. Stockmayer, J. Chem. Phys. 17 (1949) 1301.
[167] J. Mazur and F.L. Mc Crackin, Macromolecules 10 (1977) 326.
[168] J. Mazur and F.L. Mc Crackin, Macromolecules 14 (1981) 1214.
[169] D. Stauffer, Introduction to Percolation Theory, ref. [140] and H. Herrmann in ref. [141].
[170] A. Kolinski and A. Sikorski, J. Pol. Sc. Pol. Lett. Ed. 20 (1982) 177, J. Pol. Sc. Chem. Ed. 20 (1982) 3147.
[171] A. Sikorski and A. Kolinski, J. Pol. Sc. Pol. Chem. Ed. 22 (1984) 97.
[172] M. Miyake and K.F. Freed, Macromolecules 16 (1984) 1228, 17 (1984) 678.
[173] K. Ohno, in preparation (1988).
[174] S.G. Whittington, J.E. Lipson, M.K. Wilkinson and D.S. Gaunt, Macromolecules 19 (1986) 1241.
[175] J.E.G. Lipson, S.G. Whittington, M.K. Wilkinson, J.L. Martin and D.S. Gaunt, J. Phys. A 18 (1985) L 469.
M.K. Wilkinson, D.S. Gaunt, J.E.G. Lipson and S.G. Whittington, J. Phys. A 19 (1986) 789.
Recently they also analyzed star-polymers near a wall: S. Colby, D.S. Gaunt, G.M. Torrilli and S.G. Whittington, J. Phys. A 20 (1987) L 515.
[176] G.S. Grest, K. Kremer and T.A. Witten, Macromolecules 20 (1987) 1376.
[177] J.J. Freire, R. Prats, J. Pla and J. de la Torre, Macromolecules 17 (1984) 1815.
J.J. Freire, J. Pla, A. Rey and R. Prats, Macromolecules 19 (1986) 452.
J.J. Freire, A. Rey and J. de la Torre, Macromolecules 19 (1986) 457.
A. Rey, J.J. Freire and J. de la Torre, Macromolecules 20 (1987) 342.
[178] B.H. Zimm, Macromolecules 17 (1984) 795.
[179] K.E. Evans, J. Pol. Sc. Pol. Lett. 20 (1982) 103. K.E. Evans and S.F. Edwards, J. Chem. Soc. Faraday Trans. 2, 77 (1981) 1891.
[180] A. Baumgärtner and D.Y. Yoon preprint, J. Chem. Phs. 79 (1983) 521.
[181] I. Carmesin and K. Kremer, in preparation (1988).
[182] J.M. Deutsch, Phys. Rev. Lett. 54 (1985) 56.
[183] A. Sariban and K. Binder, J. Chem. Phys. 86 (1987) 5853.
[184] A. Sariban and K. Binder, Macromolecules 21 (1988) 711.
[185] (a) A. Kolinski, J. Skolnick and R. Yaris, J. Chem. Phys. 84 (1986) 1922.
[185] (b) A. Kolinski, J. Skolnick and R. Yaris, J. Chem. Phys. 86 (1987) 1567, 7164, 7174.
[186] J.D. Ferry, Viscoelastic Properties of Polymers (Wiley, New York, 1980) 3rd ed.
[187] W.W. Graessley, Faraday Trans. Symp. Chem. Soc. 18 (1983) 7.
[188] P.G. de Gennes, J. Chem. Phys. 55 (1971) 572.
[189] M. Doi and S.F. Edwards, J. Chem. Soc. Faraday Trans. 2, 74 (1978) 1789, 1802, 1818.
[190] De La Batie, Viovy and L. Monnerie, J. Chem. Phys. 81 (1984) 567.
[191] For a recent review see J. Klein, in: Polymer Handbook, to be published.
[192] S.F. Edwards and K.E. Evans, J. Chem. Soc., Faraday Trans 2, 77 (1981) 1913.
[193] J.M. Deutch, Phys. Rev. Lett. 49 (1982) 926.

[194] K. Kremer, Phys. Rev. Lett. 51 (1983) 1923.
[195] H. Meirovitch, Macromolecules 17 (1984) 2038.
[196] W.G. Madden, J. Chem. Phys. 87 (1987) 1405.
[197] E. De Vos and A. Bellemans, Macromolecules 7 (1974) 812.
[198] E. De Vos and A. Bellemans, Macromolecules 8 (1975) 651.
[199] H. Okamoto, J. Chem. Phys. 79 (1983) 3976.
[200] H. Okamoto, J. Chem. Phys. 83 (1985) 2587.
[201] H. Okamoto and A. Bellemans, J. Phys. Soc. Japan 47 (1979) 955.
[202] H. Okamoto, J. Chem. Phys. 70 (1979) 1690.
[203] H. Okamoto, J. Chem. Phys. 64 (1975) 2686.
[204] H. Okamoto, K. Itoh and T. Araki, J. Chem. Phys. 78 (1983) 975.
[205] R. Dickman and C.K. Hall, J. Chem. Phys. 85 (1986) 3023.
[206] B. Widom, J. Chem. Phys. 39 (1963) 2808.
[207] R. Dickman, J. Chem. Phys. 87 (1987) 2246.
[208] P.J. Flory, J. Chem. Phys. 9 (1941) 660.
[209] M.L. Huggins, J. Chem. Phys. 9 (1941) 440.
[210] A.M. Skvortsov, A.A. Sariban and T.M. Birshtein, Polym Sci. USSR 19 (1977) 1169.
[211] H.C. Öttinger, Macromolecules 18 (1985) 1348.
[212] K. Binder, ed., Monte Carlo Method in Statistical Physics (Springer, Berlin, Heidelberg, New York, 1979).
[213] K. Binder, ed., Applications of the Monte Carlo Method in Statistical Physics (Springer, Berlin, Heidelberg, New York, 1984).
[214] K. Binder, Ferroelectrics 73 (1987) 43.
[215] K. Binder, J. Comput. Phys. 59 (1985) 1.
[216] M.N. Barber, in: Phase Transitions and Critical Phenomena, vol. 8, eds. J.L. Lebowitz and C. Domb (Academic, New York, 1983) chap. 2.
[218] J.F. Joanny, L. Leibler and R. Ball, J. Chem. Phys. 81 (1984) 4640.
L. Schäfer and Ch. Kappeler, J. de Phys. 46 (1985) 1853.
D. Broseta, L. Leibler and J.F. Joanny, Macromolecules 20 (1987) 1935.
[219] H.G. Elias, Makromoleküle, Struktur–Eigenschaften–Synthesen–Stoffe–Technologie (Hüthig & Wepf, Basel, 1981).
[220] D. Ceperley, M.H. Kalos and J.L. Leboritz, Phys. Rev. Lett. 41 (1978) 313.
M. Bishop, D. Ceperley, H.L. Frisch and M.H. Kalos, J. Chem. Phys. 72 (1980) 3228, 75 (1981) 5538.
[221] G.S. Grest and K. Kremer, Phys. Rev. A33 (1986) 3628.
K. Kremer, G.S. Grest and I. Carmesin, preprint (1988).
[222] D. Rigby and R.J. Roe, J. Chem. Phys. 87 (1987) 7285.